Modelling of Soil-Tool Interactions Using the Discrete Element Method (DEM)

by

Steven Murray

A Thesis submitted to the Faculty of Graduate Studies of

The University of Manitoba

in partial fulfillment of the requirements of the degree of

MASTER OF SCIENCE

Department of Biosystems Engineering

University of Manitoba

Winnipeg

Copyright © 2016 by Steven Murray

Table of Contents

Abstract

Soil disturbance and cutting force are two of the most common performance indicators for soil-engaging tools. In this study the interaction of two soil-engaging tools (a disc opener for fertilizer banding and a hoe opener from an air drill) with soil were modeled using Particle Flow Code in Three Dimensions (PFC^{3D}), a discrete element modeling software. To serve the development of the soil-disc model, the disc opener was tested in an indoor soil bin with a sandy loam soil. The disc was operated at a depth of 38 mm, a travel speed of 8 km/h, and different vertical tilt angle (0°, 10°, and 20°). Draft and vertical forces, and soil disturbance of the disc opener were measured in the tests. The data were then used to validate the soil-disc model. Both the model and the experiment showed an increasing trend of soil throw with the increased tilt angle. Force results from the experiment did not have any particular trends, whereas increasing the tilt angle in the model decreased the draft and vertical forces. When comparing the model to the experiment results, the relative error was 11% for the average soil throw, 1.9% for the average draft force, and 51% for the average vertical force. To calibrate the soil-hoe model, a virtual vane shear test was created within PFC^{3D} and the output soil shear strengths were compared to measurements taken in a field with clay soil. The result showed that the calibrated effective modulus, a critical microproperty of model particles, was 5.692e7 Pa. To validate the soil-hoe model, an air drill with the hoe openers was tested in the same field at a working depth of 38 mm and a travel speed of 8 km/h. Soil throw resulting from the hoe opener was measured. Results showed a relative error of 15% between the simulated soil throw and the measured one. In conclusion, both the soil-disc and soil-hoe models could simulate the selected soil dynamic properties (except for the vertical forces of the disc opener) with a reasonably good accuracy, considering the highly variable nature of the soil.

Keywords: DEM, PFC^{3D}, disc, hoe, opener, soil, disturbance, force.

Acknowledgements

I thank Dr. Mohammad Sadek, Mukta Nandanwar, and Sandeep Thakur for their help in preparing the soil bin prior to each block of tests as well as taking measurements for soil bin testing of the disc opener. I also thank Mukta Nandanwar, Pieter Botha, and Shêne Damphousse for their aid in gathering field test data and Brian Murray of Snowy Owl Farms Ltd. for access to his fields during testing. Additionally, I thank Atom-Jet Industries and the Mitacs Accelerate program for funding this research. As well I thank Dr. Chen from the University of Manitoba for her advice during my M.Sc. program.

List of Tables

List of Figures

1 – Introduction

Soil-tool interaction is at the center of many agriculture field operations. Soil-tool interaction is also one of the fundamental aspects of soil dynamics in agricultural engineering. In a field operation, tillage tools (e.g. plows, chisels, sweeps, etc.) loosen soil for seedbed preparation, or seed openers (e.g. hoes, discs, shovels, etc.) open soil for seed placement. A general term for tillage tools and seed openers is "soil-engaging tool". The dynamic behaviors of soil determine the performance indicators of tillage and seeding, such as draft force and soil disturbance. Soil-tool systems are complex as soil consists of a matrix of discrete particles that are of random, heterogeneous nature, and exhibit sophisticated, non-linear behavior. In the field of soil dynamics, modelling of soil-tool interaction has been traditionally done using analytical or finite element models. Within these models, soil is assumed to be homogeneous, has elastic or viscoelastic behavior, and moves at small displacement. In reality, agricultural soil contains moisture, organic matter, is non-homogeneous, and moves at very large displacements during tillage and seeding operations. There is need to develop a model of soil-tool interaction that can address the complex nature of soil in agricultural fields. In recent years a new, innovative numerical method, discrete element method (DEM), has been used to develop soil-tool interaction models. In the DEM, soil is represented by discrete particles defined by a set of microproperties. The method is capable of addressing the heterogeneous nature of soil and large displacement of soil particles resulting from soil-engaging tools. DEM is able to predict soil micro-dynamics (e.g. forces and displacements of each individual soil particle) and macro-properties such as soil cutting forces and disturbance. However, defining model particles and calibrating particle microproperties is extremely challenging. In this regard progress has been limited for many years. This study has addressed some of these issues with the focus on modelling seeding tools. Interaction of a disc opener and hoe openers with soil were modelled using the DEM. The models were capable of predicting soil cutting forces as well as the soil disturbance characteristics of the openers. The results can be used to guide the design of openers which require minimum tractor horsepower and create optimal soil conditions for crop growth. The modelling approaches used in this study can be used for modelling other soil-engaging tools.

2 – Literature Review

2.1 – Soil-Engaging Tools

Agricultural Background

In 2012, the Food and Agriculture Organization released a document showing the projection of world food requirements in 2050. This document showed that the projected increase in cereal crop requirements is from 2,068 million tonnes in 2005 up to 3,009 million tonnes in 2050 (Alexandratos and Bruinsma 2012). This was an increase of approximately 45% over the production levels in 2005. Typically, a problem of food shortage would be solved by increasing the land for food production; however, this is no longer a viable solution to the problem. Every year the amount of arable land in the world decreases due to many human and climatic factors such as soil degradation, urban sprawl, and climatic shifts. As such, the objective of a great deal of agricultural improvements has been to both increase the production capacity of the currently available arable land as well as to minimize the effects of soil degradation.

At a time when world food demand, cost of energy, and environmental impact are critical concerns, Western crop production practices have shifted in the past 10 years from conventional tillage to conservation tillage, where at least 30% of plant residue is left in the field. This pushes towards low soil disturbance and low energy farming practices. As a result, the development of agricultural machines which have low soil disturbance and low power requirements is becoming increasingly important.

Types of Soil-Engagement Tools and their Functions

Soil-engagement tools refer to any type of tool that interacts with soil to mechanically alter the soil structure. This term covers a very large number of tools in agricultural engineering and in civil engineering (such as excavator buckets). With respect to agriculture, the primary types of soil-engagement tools are tillers and seeders. Each of these types has a different function and different effects on soil structure.

"Tillage may be defined as the mechanical manipulation of soil for any purpose, but usually for nurturing crops" (Srivastava et al. 2006). Tillage tools are tools which are specifically designed to break and mix the soil. These tools are typically classified into two categories, primary tillage and secondary tillage. Primary tillage tools are used to control residue from harvested crops and loosen soil such as ploughs, subsoilers, and rotary tillers. Secondary tillage tools are designed to prepare a soil bed prior to seeding such as harrows, cultivators, and rollers.

Seeding tools refer to any type of soil-engagement tool whose primary use is placing seed or fertilizer down into the soil. The general function of these tools is to fracture and loosen the soil to create an even seedbed while also placing the seed and fertilizers in locations that will not cause seed damage. In addition to fracturing, the soil seeding tools generally have a secondary tillage tool attached that runs behind the seed opener. These tools could be either harrow tines that level the soil surface, or packing rollers that compress the soil above the seedbed.

2.2 - Types of Seeding and Fertilizer Openers

Seeding implements can have a wide variety of different opener types. Despite all the potential variations between drills and planters, all openers perform the same functions. An opener must be able to break apart soil, create a furrow, and place seeds or fertilizer into the created furrows. There are three most common types of seed openers: shovel openers, disc openers, and hoe openers.

Shovel openers were common in the first generation of air seeding implements. A shovel opener is a cultivator sweep with a seed or fertilizer tube that deposits product down behind the sweep. Sweep wings are upwards of 203.2 mm wide and cause high soil disturbance. Various shovel openers are still in operation throughout Europe as these openers perform well in moderate residue conditions. However, these openers have been phased out of use in North America due to the progression away from conventional tillage practice in favor of low soil disturbance.

Disc openers perform in the opposite fashion to shovel openers, in terms of soil disturbance. While shovels were made to disturb a significant amount of soil to put down a large amount of product, disc openers create very narrow furrows to accurately place a smaller amount of product. Disc drills are typically designed to have narrow row spacing (such as 190 mm) due to their minimal lateral soil disturbance. Disc openers operate with a very low gang angle (< 10°), which allows them to have low pulling force requirements as well as minimal soil disturbance. This type of openers is most suitable in no-tillage and conservation tillage systems.

Hoe openers are the most common type of opener currently used on air seeding implements in Western Canada (Chen et al. 2004). The popularity of these openers comes from the fact that they can be tailored to suit many different applications. They vary from single shoot fertilizer application knives up to four or five shoot openers capable of placing seed, granular fertilizer, NH_3, liquid fertilizer, and starter nutrients. The versatility of hoe openers allows them to be used for a single pass application style of crop production which in turn limits the amount of soil degradation from multiple passes of agricultural equipment. Due to the potential complexity in the designs of hoe openers, there can be significant drawbacks due to their high cost.

Each type of opener has its advantages and disadvantages. In terms of soil disturbance, disc openers disturb soil the least (Janelle et al. 1995; Parent et al. 1993), and therefore they have been used more often in no-tillage systems than any other opener types (Baker et al. 1996). Disc openers also require the least draft force to pull and will not plug in taller stubble (Green and Poisson 1999). Hoe openers cost more to manufacture, are more versatile and have higher precision of seed placement (Darmora and Pandey 1995; Doan et al. 2005). Shovel openers disturb more soil, but can handle certain amounts of residue on the field. More information about comparisons of different openers can be found in Chaudhuri (2001). This study focused on a disc opener and various hoe openers.

2.3 - Performance Indicators and Evaluation

The typical performance indicators for openers have four categories: soil effects, seed and fertilizer placement, soil cutting forces, and crop response. Each performance indicator has its own methods for measurements as well as its impact on design consideration. The following sections describe only soil effects and cutting forces, which were the focus of this study.

Soil Effects

Of all the performance indicators, soil characteristics resulting from an opener are considered one of the most critical performance indicators. Soil characteristics include soil throw in lateral and vertical directions, soil bulk density, furrow profile, and surface roughness. This study focused on soil throw characteristics, as this characteristic has been considered to be one of the most critical performance indicators in opener evaluation (Hasimu and Chen 2014). Soil throw is directly associated with soil stepping which is when an opener on a trailing rank throws soil onto the furrow of a leading rank. Soil stepping is undesired, as it leads to uneven soil coverage on seeds and uneven crop growth. Ideally, an opener would allow the disturbed soil to fall directly back into the furrow; however, this is nearly impossible. An opener is designed to keep lateral soil throw minimal to avoid soil stepping. In summary, information on lateral soil throw will aid in the design of openers, and guide the opener arrangements on seeders.

While lateral soil throw is a critical performance indicator, soil vertical throw height also plays a large part in the evaluation of openers, especially hoe openers that are designed with either a large rake point or a vertical point (90º rake angle). Openers with smaller rake angles cut through the soil and lift it over the opener, whereas openers with large rake angle or vertical points fracture the soil ahead of the opener. This is why these points are generally made of hardened steel as they absorb the majority of the force of the soil-tool contact. If the soil vertical throw height is large, soil rides up the point and eventually contacts the opener boot which is generally made of a mild steel. This leads to significant wear on the opener boot.

Forces on Openers

Soil cutting forces are also important performance indicators of openers or other soil-engaging tools (Collins and Fowler 1996; McKyes 1985). As seeders increase in size, it becomes increasingly important to reduce the forces the openers require for operation. The force components of the openers break down into the draft force, vertical force, and lateral force. Draft force is the force required to pull the opener through the soil, vertical force is a measure of the opener's ability to either force itself out of the ground or further down into the soil, and lateral force is the amount of side loading on an opener as a result of an asymmetrical design. Both draft force and vertical force are determining factors for choosing a tractor of the smallest horsepower that is required to pull a specific seeder. The draft force of an opener is a measure of the additional horsepower beyond the rolling requirements of the seeder that the tractor requires to pull the openers through the soil. While lateral force does not directly relate to the tractor requirements of an implement, it is critical in the design as opener shanks are typically designed to handle loads applied in the draft and vertical directions and be able to transfer them through to the implement frame. Extra lateral forces can cause openers to twist on the machine shanks.

Soil cutting forces and soil disturbance are important performance indicators of seed and fertilizer openers. Therefore, an optimal opener has the smallest soil cutting forces in all three directions and minimum soil disturbance. Soil disturbance and soil cutting forces are affected by many factors such as the travel speed, working depth, and geometry of the opener (Gratton et al. 2003). Of all factors, opener geometry can be most easily modified to minimize soil disturbance and cutting forces.

2.4 - Modelling of Soil-Tool Interactions

Modelling of soil-tool interaction is required to better understand soil dynamic behavior resulting from soil-tool interactions, including particle-particle interaction forces, particle-tool interaction force, as well as displacements of soil particles. The knowledge of these soil dynamic behaviours is important for the design of a soil-engaging tool that minimizes power requirement and creates optimal soil conditions for seeds and plants (Conte et al. 2011; Tamet et al. 1996; Rathore et al. 1981).

Modelling Methods

Modelling of the soil-tool interactions has been done using three methods: empirical methods, analytical methods, and numerical methods. Empirical modelling of soil-tool interaction refers to building a generalized model based on experimental results. For example, Liu et al. (2008) and Rahman et al. (2005) collected soil movement data of sweeps from an indoor soil bin and correlated the data with the tool geometrical and operational parameters. The empirical relationships can be used for prediction of soil movement in other applications. Empirical methods are time consuming as they require collection of a large amount of data. Most empirical models do not have good accuracy as data is highly variable due to the non-homogeneous nature of soil.

Analytical models are based on Coulomb's passive pressure theory and assumption that soil will fail in a certain path, for example, from the tip of the cutting tool up to a point at the soil surface some distance ahead of the tool, i.e. wedge failure (McKyes 1985). Using Coulomb's work in combination with the Mohr's circle for calculation of plane stresses, a universal earth moving equation was generated. Several versions of the universal earth moving equation have been developed (Hettiaratchi et al. 1966; Godwin and Spoor 1977; McKyes and Ali 1977, McKyes 1985). The equation predicts cutting force of a soil-engaging tool and the soil cross-sectional area disturbed by a tool, as the functions of soil weight of the failure wedge, soil internal friction and cohesion, soil-tool adhesion, and tool working width. The tool working parameters, including rake angle and working depth are also taken into account in the equation. While analytical models are useful for the calculation of basic soil-tool interactions, they are limited by a number of factors. One is the assumed soil failure pattern, which is not always true as soil failure resulting from a soil-engaging tool has random patterns. The other limitation is that the analytical method is only suitable for a simple tool, such as a blade. Their usefulness diminishes upon the addition of complex geometry as seen on hoe openers such as wings and chutes. In addition, the method cannot be developed for rotary tools, such as discs.

To analyze the increasingly complex geometry of seeding and tillage tools, numerical models such as finite element analysis (FEA), computation fluid dynamics (CFD), and discrete element modelling (DEM) have been used. Chi and Kushwaha (1990) developed a model using FEA to study the soil failure under loading from a simple tillage blade. This model was capable of predicting the draft and vertical forces on a simple tillage tool at rake angles between 30 and 90°. The model was also able to accurately predict the shape of the soil shear stress region ahead of the tool. Several other researchers (e.g. Plouffe et al. 1999; Upadhyaya et al. 2000) have also developed soil-tool interaction models using FEA. The drawbacks of this method include that FEA deals with only a continuous medium, i.e. soil displacement has to be small (Abo-Elnor et al. 2004). In practice, soil particles have large displacements in all directions during a field operation. Rahman et al. (2005) reported that a sweep travelling at 5 km/h could move soil particles distances of 83 mm vertically, 273 mm laterally, and 937 mm forwards. Such large displacements cannot be modelled using any traditional modelling methods. Another limitation of the analytical method and FEA is that they cannot predict soil behaviours at particle level. They only account for total soil deformation and force of a soil body. More recently, a study by Karmakar, Kushwaha and Laguë (2007) aimed to use CFD software to analyze the interaction between soil and simple tillage tools. In that study, the motion of the tool through the soil was simulated by locating a stationary tool within a constant flow of soil. The model was capable of displaying pressure distributions around the tool. The feasibility of using the CFD for modeling soil-tool interaction require further studies, as soil is more a granular material in nature than a fluid. The DEM has been lately used for simulation of soil-tool interactions. The advantages of this method over other methods include its capability of addressing the discontinuous nature of soil flow around tools, large particle displacement, and complex tool geometry. This method is further discussed in the following sections.

2.5 - Discrete Element Method (DEM)

The discrete element numerical method treats all parts within the model as discretized elements. First introduced in 1979 (Cundall and Strack 1979), the discrete (distinct) element method describes the mechanical behavior of a model assembly composed of discs (2D) and spheres (3D). Elements are capable of translating and rotating individually to simulate particle based medium and the interaction with the environment. In the DEM, material is modelled as discrete particles. Particles are given specific properties (named microproperties of particle), and the contacts between particles are governed by certain constitutive laws, so that the contact behaviours of the model particles reflect the behaviours of the material to be simulated. The DEM was first introduced in the field of soil and rock mechanics. DEM has since been used in many applications such as modelling the flow of grain from a silo (Lu, Negi and Jofriet 1997), application of manure (Landry 2006), and kinematics of void collapse (Lim and McDowell 2008). More recently, the DEM has been used to simulate agricultural soil-engaging tools and their interaction with soil (van der Linde 2007; Fielke et al. 2013; Sadek and Chen 2015) and interaction of soil with animal claws (Li et al. 2015).

Application of the DEM in Soil Dynamics

As soil is a particle based medium, the discrete element model is a proper fit for analyzing the interactions between soil and tillage tools. When using the DEM to simulate soil-tool interactions, the soil domain is treated as an assembly of individual particles. As the tool travels within the soil domain, individual soil particles are being impacted, and each particle contacts with its neighboring particles, resulting in particle displacements and contact forces of particle-to-tool and particle-to-particle. Particle laws (defining particle contact behaviours) and microproperties of soil particles determine the macro-behaviours of the soil.

Previous soil-tool interaction models have included a soil-subsoiler model (van der Linde 2007) where it was found that the DEM was able to help explain why a vibratory subsoiler would decrease the required draft loading. A soil-blade model has been developed and calibrated using the DEM for two different contrasting soil types (Mak et al. 2012), and the simulated soil cutting forces were comparable with those predicted using the universal earth moving equations. The soil-sweep model developed by Mak and Chen (2014) was also able to simulate soil cutting forces, which matched reasonably well with measurements. These earlier models focused on force predictions, as DEM software had prebuilt functions for monitoring soil-tool contact forces in all three directions. Later models dealt with monitoring soil disturbance resulting from soil-engaging tools, which was more difficult than monitoring soil cutting forces. In a soil-sweep model, Tamás et al. (2013) monitored a simple soil disturbance characteristic, soil loosening, which is defined by change in soil porosity. Chen et al. (2013) simulated soil disturbance in more detail. They monitored soil surface and furrow characteristics resulting from a sweep. Tanaka et al. (2007) developed a DEM model to predict soil loosening and cracking generation caused by a vibrating subsoiler. The most recent model simulated soil surface roughness and soil cover depth (Gao et al. 2015). However, further research is required to model other soil disturbance characteristics, such as soil throw distance by openers which is much more useful for the design of tool geometry, selection of the material strength, and wear properties of the tool.

2.6 - Particle Flow Codes in Three Dimensions (PFC^{3D})

The discrete element method has evolved into several commercial software packages, one being Particle Flow Code (PFC). PFC is a general purpose discrete element modelling software created by Itasca Consulting Group, Inc. (Minneapolis, MN). PFC is available for use in either two dimensions or three dimensions. This software is used for simulation of particulate interactions in many applications from analyzing the efficiency of mixing particles within a drum to measuring the impact forces of rock slides.

At its most base level, PFC^{3D} simulates the interactions of many finite-sized particles (Itasca 2015). Simulation models are made up of two base elements: walls and balls. Walls are capable of only interacting with the balls, while balls are also able to interact with other balls. Both balls and walls can be assigned attributes ranging from the more basic properties such as shape and size, to the more intricate properties, such as rotational and translational velocities. The framework utilizes iterative solving mechanics where each iteration is referred as a cycle. In addition to being a computational discrete element modelling software, the PFC framework includes a graphical user interface that can give both observational and graphical feedback on the simulation model.

In modeling soil-tool interaction, balls are used to represent soil particles, and walls are used to construct soil-engaging tools. Once a desired set of model walls and balls has been generated for a task, particles must be assigned contact properties. These contact properties affect the interaction of elements within the model. The PFC framework contains ten built-in contact models that can be used to describe most types of mechanical interactions. For example, the parallel bond model allows adding bond between particles in contact (Potyondy and Cundall 2004). Bonds act as a type of epoxy, cementing two particles, which reflect the cohesive behavior of soil aggregates. Bonds in the model are specified with strength and capable of transmitting forces between particles and resisting relative rotation. Bonds break when the external force exceeds the perspective strength, which mimics soil breakage under a soil-engaging tool. If the user decides that none of the prebuilt models are appropriate, there is also the option to create a user-defined contact model. As such the software is capable of simulating a large range of materials, from cohesive to cohesionless, and from granular to solid material.

In addition to assigning a contact model to a simulation, its effectiveness should be also determined. The user must determine the parameters that cause the model to behave as close to reality as possible. These parameters are known as particle microproperties. Within each contact model, there are numerous microproperties that affect the model output. For example, within the linear contact model, there are nine modifiable microproperties, and in the linear parallel bond model (LPBM) there are 18 microproperties that are separated into three groups, the linear group, dashpot group, and parallel-bond group and several modifiable microproperties exist within each group (Itasca 2015). Particle microproperties are not measurable owing to their micro scale, therefore they must be calibrated.

2.7 - Microproperties Calibration and Model Validation

Microproperties of soil particles determine the macro-behaviours of the soil. A discrete element model can be successful only if its particle microproperties are defined correctly. There are many microproperties, and they cannot be calibrated at the same time. Some of the values must be assumed logically and adapted from the literature. The macro-behaviour of the material to be modelled is considered to be determined collectively by those microproperties (Potyondy and Cundall 2004). However, some microproperties are more critical than others, and those critical microproperties should be calibrated. In studying soil shear properties using PFC, Nandanwar (2015) reported that the particle friction is the most critical microproperty to determine soil shear strength. A study by Sadek et al. (2011) found that the particle stiffness and bond normal stiffness within the LPBM model had the most significant change on the measured yield forces during a simulated soil shear test. It was also noted that the particle friction coefficient showed no significant effects on the results, which was inconsistent with a simulation study on shear properties of corn (Coetzee and Els 2009). The study found the shear forces to be highly dependent on particle friction. In another study, the effects of many microproperties on soil throw were tested for a simple soil engaging tool (Sadek and Chen, 2015). From that study, feasible ranges for soil-tool interaction models were found for critical parameters of the LPBM. These parameters included the particle modulus of elasticity, bond modulus of elasticity, bond strength, local damping coefficient, and viscous damping coefficient. The study found that within these ranges the soil-tool interaction behavior was found to be representative with respect to experimental soil bin testing. In summary, it is important to examine which microproperties are critical to the model outputs of interest.

Once the critical microproperties are identified, calibrations of those microproperties can be done using soil mechanical tests, such as triaxial tests (Nandanwar 2015), direct shear tests (Sadek et al. 2011), and penetration test (Mak 2011). These methods have been considered to be effective, as good agreements have been reported among simulations, theories, and measurements.

2.8 - Use of Simulations for Opener Design

Extensive testing is required on new iterations of prototypes before they are ready to be marketed to the consumer. A difficulty arises when testing seed openers for their field performance as field tests can only be performed once a year in most climates during the spring while seeding. This leaves the bulk of the year where full scale field testing is not viable, leaving only the option for laboratory or small field patch tests. For laboratory testing, a soil bin is required and it is not always available. Therein lays an inherent issue, when a flaw in a design is noticed, the next iteration must wait an entire year before it can be tested in field conditions, which leads to long design schedules and delays in product releases. With the continued increase in computing power available to researchers and engineers, high precision simulation software is becoming increasingly available for use during the design process. Recently, DEM software such as PFC^{3D} has been utilized increasingly to help model situations where soil or other particle-based mediums are one of the interacting bodies. Simulations allow engineers to bypass the climatic limitations placed on testing. By simulating potential prototypes in a model, engineers would be able to virtually test potential design ideas throughout the entire year, and also allow more accurate testing of the effects of minor design changes such as wing or point angles for optimal performance. Despite the significant increase in readily available and cost-effective high resolution and high frame rate cameras on the market, slow motion video results of field operation or soil bin operation leaves data collection as primarily observational within the seeding and tillage sector. Utilizing the power of simulation, modelling allows the engineer to gather quantitative results in a field typically focused on observation. Simulations can also be used as a tool to focus field testing. If an engineer was to bring several prototype ideas to a simulation model, the simulation results could be used to eliminate some of the prototype ideas thus allowing a more focused set of physical prototypes to be built for field testing saving the company both time and money. Lastly, utilizing the simulation model for soil-tool testing allows the engineer to test the prototype designs within different types of soils.

While there are numerous benefits to the use of DEM in terms of design of prototype openers, the program is not without drawbacks. Due to the large number of discrete elements that can exist within a DEM simulation, a single simulation step can require thousands of computations. Such a large number of computations can require highly expensive computers for such simulations. In addition to the large computer requirements, simulations that utilize a large number of elements can take days or weeks to compute thus limiting the use of the program. Lastly, due to the number of microproperties that can be calibrated within the program, results from a simulation must be interpreted with caution as a set of calibrated properties refers to only a very specific calibrated soil type.

In summary, openers are the major soil-engaging tools of seeding equipment. Common types of openers include discs for conservation tillage systems and hoe openers for high precision seeding. Soil disturbance and cutting forces are important performance indicators of openers. To study these dynamic properties, modelling approach is found to be more effective. PFC^{3D}, which utilizes the Discrete Element Method (DEM) has been recognised as an effective modelling tool. Although a significant amount of PFC^{3D} simulations have been devoted to monitor soil cutting forces and calibrate model parameters, there was limited information on soil disturbance. All these justified the aforementioned objectives of this study.

3 – Objectives

The objectives of this study were to (1) develop models to simulate soil-disc and soil-hoe interactions using PFC^{3D}, (2) calibrate and validate the models using laboratory or field measurements, and (3) use the models to predict soil properties (soil disturbance and cutting forces).

4 – Methodology

4.1 - Disc Opener

Soil Bin Tests of a Disc Opener

Description of the Disc Opener Experiment was conducted on a disc opener for dry fertilizer application. It was a plane disc and had a diameter of 305 mm with a flat cutting face (Fig. 1a). The disc was sharpened on one side, i.e. tapered on the back down to a diameter of 295 mm over a depth of 7.5 mm (Mahadi 2005) (Fig 1b). Testing was performed in the Soil Dynamics and Machinery Lab in the University of Manitoba. The testing facility was a 10.0 m long, 1.0 m wide, and 0.6 m deep soil bin (Fig. 1c). The opener was attached to a shank using four carriage bolts that could be adjusted to alter the disc's tilt angles. The shank was then attached onto the soil bin plate dynamometer using the four attachment bolts on the plate. The soil was a sandy loam soil (70% sand, 16% silt, 14% clay). For the experiment, a four stage procedure for soil preparation (spraying water, cultivating, leveling and compacting) (Hasimu and Chen 2014) was followed.

(a) (b) (c)

Figure 1a - Tested disc opener. Figure 1b - Beveled cutting edge of the test disc. Figure 1c - Soil bin used for physical testing.

Experimental Design To examine effects of the tilt angle of the disc (Murray 2014), a randomized block experiment was designed with three treatments: 0, 10, and 20° tilt angles and 3 blocks. Each block contained one trial run at each angle. The disc gang angle used was 10º, the working depth was 37.5 mm, and the travel speed was 2.22 m/s (8 km/h).These operational parameters were kept constant for all test runs.

Measurements Before the tests, soil samples were taken from the soil bin to ensure that soil bulk density and moisture content remained similar throughout each of the three blocks. Prior to each trial block, three soil cores with a 50 mm diameter and 50 mm height were taken from the soil bin at random locations. The samples were weighed, oven-dried for 24 h at 105°C, and weighed again to determine the soil moisture content (d.b.) and dry bulk density (ASABE Standard 2012).

During each test run, the draft, vertical, and lateral forces of the disc were monitored with a plate dynamometer mounted between the disc hitch and the soil bin carriage (Fig. 1c). The signal of the dynamometer was recorded with a Campbell Science data logger (Campbell Scientific Inc., Logan, Utah) and a computer at 35 Hz. The force of the test run was the average of the data points within the constant velocity section of the disc.

Figure 2 - Soil throw distance measurement technique.

After each test run, soil throw distance was measured to quantify the soil disturbance of the disc. After passage of the disc, a rope was laid along the far edge of the thrown soil (Fig. 2). The lateral distance between the rope and the center of the created furrow was measured at seven predetermined locations within the constant velocity section of the disc. The average of seven data points was reported as the soil throw distance of the run.

Data Analysis Analysis of variance (ANOVA) was performed using a statistical analysis software version 9 (SAS Institute, 2013). Duncan's multiple range tests were used to detect statistical significance of treatments.

Development of Soil-Disc Model

Model Specifications The soil-disc model consisted of a model soil bin, filled with model soil particles, and a virtual disc (Fig. 3). Using PFC^{3D} 5.0, a model soil bin was created to emulate the conditions seen during experimental testing. Dimensions for the model bin were chosen with the goal of minimizing the required particle count while still allowing for stable model results. Dimensions of the model bin were chosen as 400 mm wide, 600 mm long, and 300 mm high. The width of the model bin was chosen to be slightly larger than the observed soil throw distance during experimental testing. The length of the model bin was chosen to allow the disc to have a constant velocity zone of 200 mm to monitor the cutting forces and soil disturbance.

Particles to be generated in this model were chosen to be spherical and had a 5 mm diameter, as this value represented the soil bin soil while maintaining an acceptable computational load. The linear parallel bond model implemented in PFC^{3D} (Itasca 2015) was used to describe the particle contact. The microproperties of the model particles for the sandy loam soil in the soil bin have been calibrated by Sadek and Chen (2015), and their values were used in this study (Table 1). Particles were generated in three batches of 100,000 particles each and allowed to settle under the influence of gravity for 25,000 cycles each. Generating the particles in batches rather than all together decreased the overall time required for generation. Once all 300,000 particles were generated, the model was allowed to settle again until the average mechanical energy in the system was lower than 0.001 J, meaning the particles were in a stable condition. Once the mechanical energy criterion was reached, generated particles that rested above the 100 mm level were deleted to create a level soil surface. A total of 228,978 particles were left in the model bin for the simulation.

Table 1 - Soil-disc model particle microproperties as per Sadek and Chen (2015).

Parameter	Value
Particle modulus of elasticity (E), Pa	2.5e5
Particle friction (μ)	0.5
Bond modulus of elasticity (Ē), Pa	2.5e7
Bond normal and shear strength (σ), Pa	2e4
Viscous damping coefficient (β)	1.0
Local damping coefficient (α)	0.5

A virtual disc (Fig. 3) was constructed to have the same dimension as the disc tested in the soil bin. The real disc had two flat surfaces and a straight bevel, which could be considered to be a truncated cone. Such a shape could be formed using the conical wall function built in PFC^{3D} 5.0. The portion of the cone lied in between two parallel planes spaced 7.5 mm apart, which was the thickness of the disc. The two parallel planes had diameters of 305 and 295 mm. As the real disc in the test threw more soil to one side due to the gang angle, the virtual disc was positioned off the center line of the model soil bin, so that a smaller model soil bin could be used while still avoiding the edge effect from the bin walls.

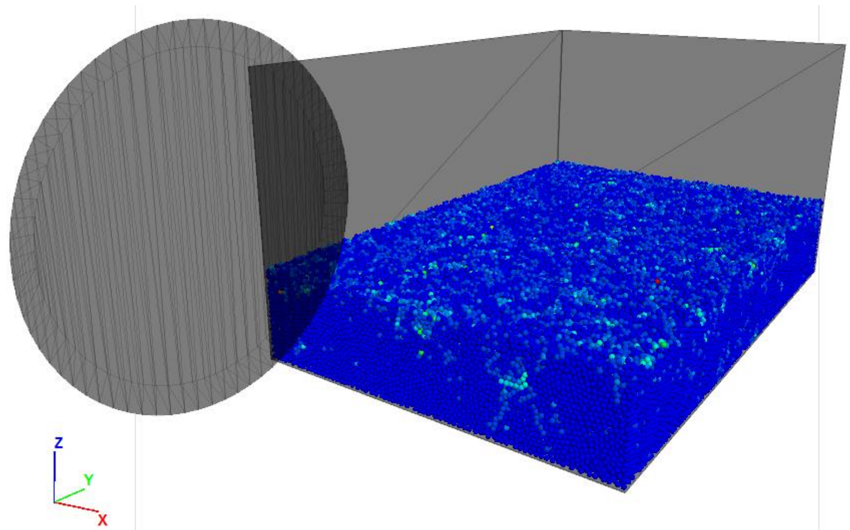

Figure 3 - Model soil bin and disc prior to simulation.

In practice, disc is mounted to a shaft through a bearing. During field operation, the disc traveled at a linear speed pulled by a tractor. At the same time, the disc rotated freely around the shaft as a result of soil resistance to the disc. This arrangement was referred to as ground-driven. In PFC simulation, the linear speed of the disc could be easily set to any value. However, the ground-driven phenomenon could not be realized in PFC^{3D}. Thus, the virtual disc was specified with a rotational speed, in additional to a linear speed. The linear speed of the virtual disc was the same as the travel speed of the real disc in the soil bin tests, and the rotational speed of the virtual disc was 14.6 rad/s, which was derived from the linear speed of 2.22 m/s and the disc radius of 0.153 m. This implied the assumptions that the disc had a zero slippage and a rotational radius that was equal to the disc radius (0.153 m).

As the virtual disc rotated and moved forward, soil particles were dislodged by the disc, resulting in the particle movement in forward, upward, and lateral direction. This behavior reflected what occurred in the soil bin tests. In a similar approach to the plate dynamometer used for measuring the forces on the physical disc during a simulation run, curves of the draft, vertical, and lateral forces on the virtual disc were recorded over time. Typical curves for a simulation run are shown in Fig.4. The simulated forces were taken as the averages over the stable sections of the curves.

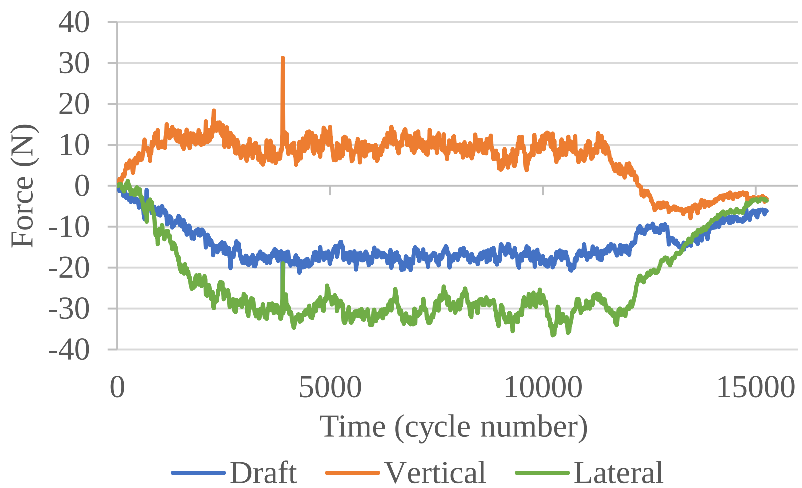

Figure 4 - Sample output from PFC^{3D} history function.

After the model had finished running, the soil throw distance was measured at 50 mm increments starting from 200 mm down the operation path and continuing through 400 mm. At each measurement location a cross section was taken (Fig. 5) along the x-axis (lateral direction) with the particles set to display the ball displacement in the x-direction. From this cross section the particle furthest away from the furrow but still in the bulk throw region was selected. Using the built-in particle property function, the location data of the particle was displayed. The x-axis location of the particle was then used as the soil throw distance for that measurement location.

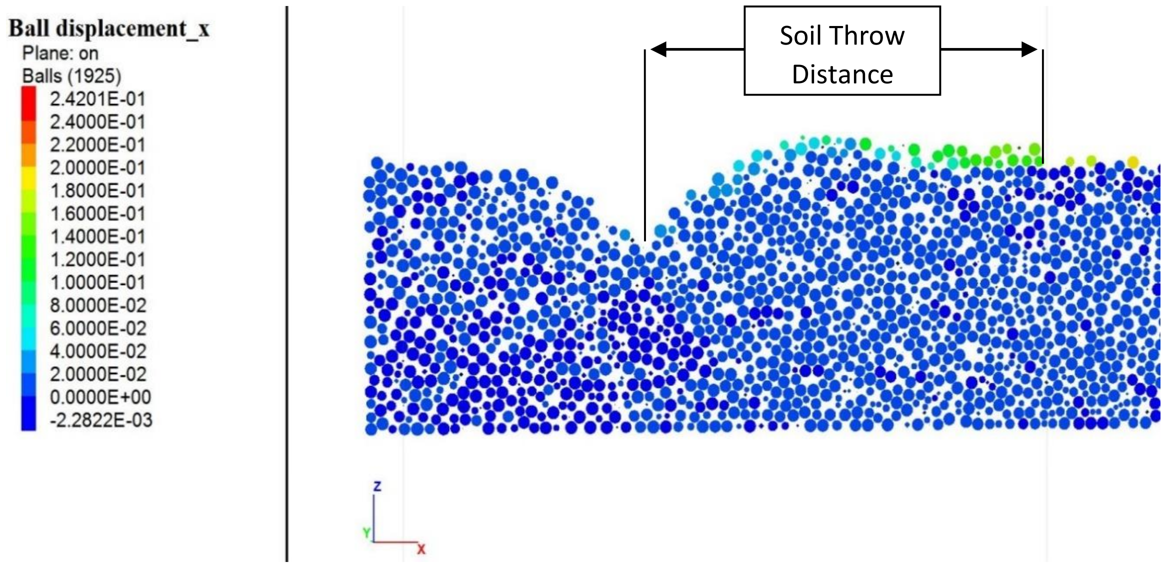

Figure 5 - Sample output of lateral cross sections used to calculate the soil throw distance.

Model Validation To validate whether the soil-disc model results were in line with the results from the experimental data, the microproperties listed in Table 1 were input into the model. During the running of the simulation, the draft, vertical, and lateral forces of the virtual disc were monitored over the length of the model soil bin. After the model had finished running, the soil throw distance was measured. The results from simulations were then compared to those found from the soil bin experiment.

Model Application The same soil-disc model as previously validated was applied to two sets of simulations. One set was to examine effects of gang angle on forces. The gang angle of the disc was changed from 0 to 30° at 5° intervals, and a constant working depth of 37.5 mm was used. The other set was to examine effects of working depth on forces. The working depth was altered from 12.5 to 75 mm in 12.5 mm intervals, and a constant gang angle of 10° was used.

4.2 - Hoe Opener

Field Tests of a Hoe Opener

Description of the Field and Hoe Opener Tests were conducted using a 12.2 m Concord air drill with 0.25 m row spacing (Fig. 6a). The seed openers on the drill were a single shoot spread opener (Atom-Jet Industries Edge-on 0.10 m) (hoe type opener). This style of seed opener (Fig. 6b, 6c) had a 25.4 mm wide point that was angled back 9.5° from vertical to shatter the soil during operation rather than lifting the soil as a positive rake point does. To create the furrow these openers had two 38 mm wings that act on the same plane as the bottom of the point.

(a)

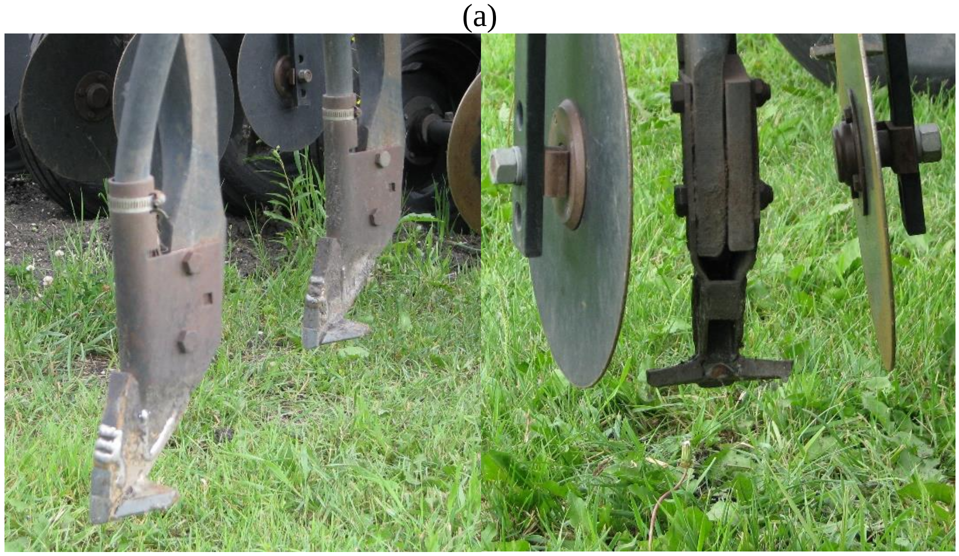

(b)

Figure 6a - Concord 4010 air-drill. Figure 6b - Atom-Jet Industries Edge-On single shoot spread openers.

Testing was performed in two fields (49.750247, -97.458906) located southwest of Winnipeg, in Sanford, MB (Fig. 7a). The soil was a clayey lacustrine soil consisting of approximately 63% clay, 28% silt, and 9% sand (Land Resource Unit 1999). The primary test field was a rectangular, 80-acre field. This field had a very distinctive low and wet area at the southwest corner, a high and dry area at the southeast corner, and average elevation and soil moisture along the entire northern (top) edge. These areas show up as the dark section with little green, a highly green section, and a mixture of green and black, respectively. The secondary test field was a long, narrow, 65-acre field (Fig. 7b). This field had a low and wet area on the eastern (bottom of image) edge, an elevated and dry area on the southern (left side of image) half of the field, and average elevation and soil moisture content on the northern side of the field.

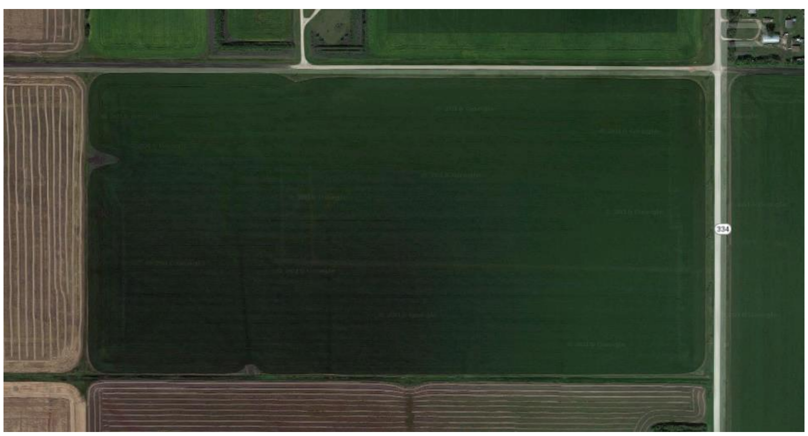

(a)

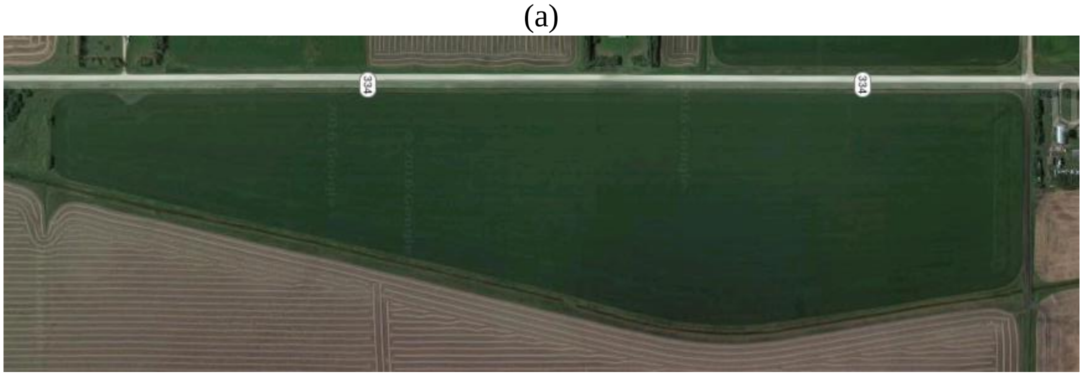

(b)

Figure 7a - Primary test field (Imagery ©2016 Google, Map data ©2016 Google). Figure 7b - Secondary test field (Imagery © 2016 Google, Map data © 2016 Google).

Field Operation and Measurements The air drill was set to maintain a constant seeding depth of 38 mm and travel speed of 2.22 m/s (8 km/h). Seeding for both fields was completed on the same day, and all operational parameters were kept the same between fields. In order to gather field data to represent the entirety of the field conditions, two random areas in each of the aforementioned high, average, and low zones in each field were chosen. Within each random test area, five replicates were taken for each measurement.

Soil cores with a 50 mm diameter and 50 mm height were taken from the field at random locations. The samples were transported back to the lab to be weighed, oven-dried for 24 hours at 105°C, and weighed a second time to determine the soil moisture content on a dry basis and the dry bulk density. In close proximity to the random soil core locations, a Geotechnics Geovane vane shear meter (Geotechnics, Auckland, NZ) was used to measure the soil shear resistance. The meter featured four vanes, a rod and a head dial (Fig. 8a). The vanes were 16.5 mm wide, 50 mm high, and 2 mm thick. To measure soil shear resistance, the vanes were vertically inserted into the soil until the tops of the vanes were flush with the soil surface. Then, the meter was rotated at a rotational speed of approximately 1 rpm until the soil failed. The reading from the dial was recorded as the soil shear resistance (torque). Additionally, a pocket penetrometer (Model No. HM-502, Italy) was used to measure the soil penetration resistance (Fig. 8b). To record the amount of trash coverage in the field, a 30.5 m rope with a tick mark every 0.3 m (a total of 100 marks on the rope) was stretched out randomly within the test areas. The number of times a piece of trash on the soil surface directly intersected a mark on the rope was recorded. The average of these recordings was taken as the trash coverage percentage. Soil throw in the lateral direction was measured on the outer opener of the drill after it had passed through the field. The soil throw was measured as the distance between the center of the furrow and the outside edge of the bulk throw.

(a) (b)

Figure 8a - Geotechnics geovane for soil shear resistance testing. Figure 8b - Pocket penetrometer for soil penetration resistance testing.

Development of a Soil-Hoe Model

Model Specifications A soil-hoe model was constructed using PFC^{3D} 5.00.23 to simulate the operation of the openers used in field testing. Initial constraining walls were created as a model soil bin with dimensions: 400 x 600 x 200 mm, leaving the top of the bin open to allow for particle generation. Particles generated into this model were chosen to be spheres with a 5 mm diameter. Particle-particle contacts were described using the linear parallel bond model (Itasca 2015), and particle-wall contacts were described using the linear model (Itasca 2015). Particles were generated and settled in the model soil bin in the same fashion as in the soil-disc model. Following deletion, a total of 229,050 particles remained, and were assigned their microproperties.

Once the soil bin had been created and finalized, a 3D CAD model of the previously tested hoe opener was created using Autodesk Inventor Professional 2016. This CAD model was then imported into the soil-hoe model using a built-in PFC^{3D} function that generates walls based on STL file input (Fig. 9). The generated CAD model was simplified from the real opener to eliminate extremely small facets in the model opener. This was done to reduce the computation time as PFC^{3D} calculates how far a wall can translate each timestep based partially on the size of the smallest facet. Several smaller features of the opener such as the hardsurface patterns (weld beads on opener sides and point) seen on the openers to trap soil and extend opener life were also omitted to obtain a level of computing time deemed affordable. However, all major soil interaction features such as the point, wings, and opener boot were kept identical between the real and model openers so that simulation results would be as accurate as possible. The generated opener was located to run along the center of the soil bin at a desired depth and a desired travel speed.

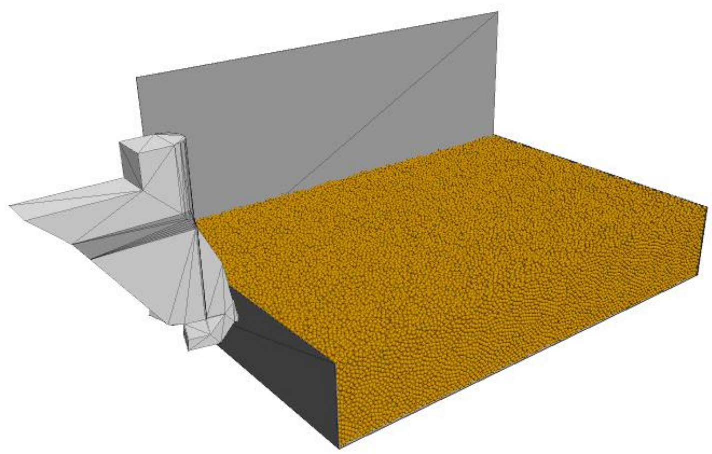

Figure 9 - Soil-hoe model state prior to model operation.

Monitoring of Dynamic Soil Properties History files were created to record the total contact forces between the particles and the opener in the X, Y, and Z directions, which corresponded to the lateral, draft, and vertical forces of the opener respectively. The simulation was allowed to cycle until the opener had passed through the bin and any disturbed particles had come to rest. Force history values were recorded every 10th cycle during operation for a total of 120,000 cycles (Fig. 10). Due to the irregularities seen in the beginning and ending sections, only the section between 20,000 and 100,000 cycles were considered to determine the average forces of a simulation run. This section was where the opener was fully inside the model soil bin and any interactions with the bin walls had no effect on the results.

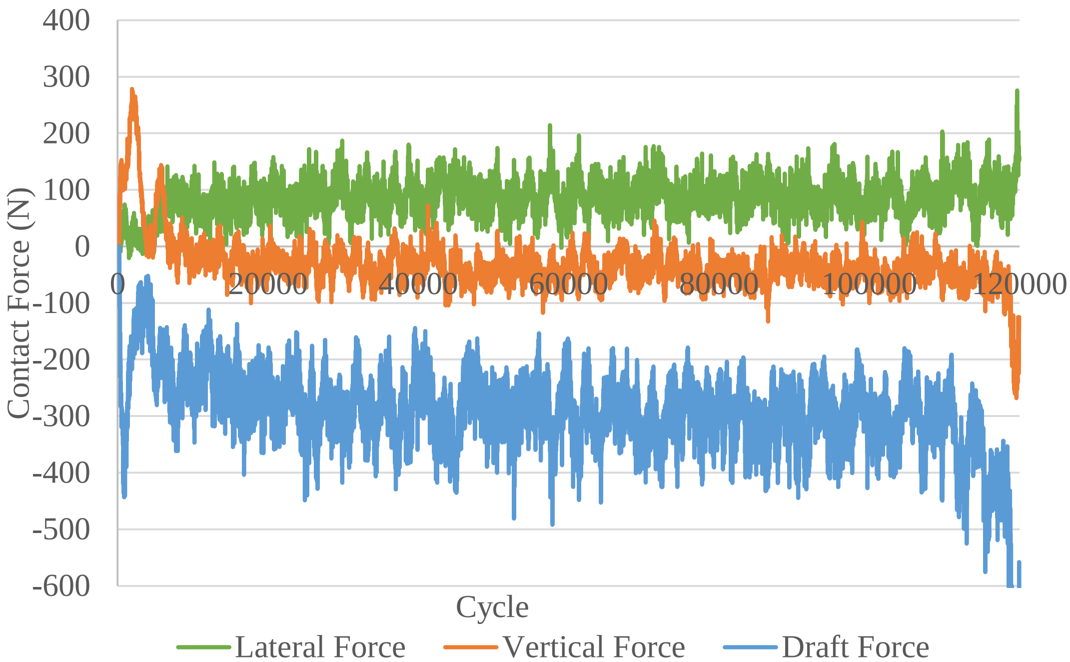

Figure 10 - Sample force output from model history function.

The lateral throw distance of the particles was measured after the opener had passed through the model soil bin. The slice (Fig. 11a) shows a soil cross-section with a furrow resulting from the model hoe opener. These slices give very valuable observational and numerical data about the soil disturbance of the opener. Each slice was 10 mm thick. Particles within the image are white before the tool operation and change to orange once they have been disturbed by more than 5 mm in magnitude of particle displacement. The change criterion was arbitrarily selected to differentiate disturbed and undisturbed soil particles. Using the built-in *measure* function, the distance to the outer edge of the bulk throw section was measured on each side of the furrow and added together to find the total lateral throw distance. Outlier particles were omitted from the soil throw measurement as in the field measurements. This measurement was taken across the bin at 25 mm intervals between 200 mm and 400 mm along the line of travel. The height of vertical soil throw was measured using the built-in *measure* functions and screenshots of the side view of the soil assembly. By utilizing the *filter* and *clip box* functions within PFC^{3D}, a view of the soil bin was created where all the particles from the center of soil model bin to one side of the bin were hidden. Additionally, wall facets were hidden in the same area so as to show a cross-section of the soil model bin along the axis of travel. This view was used to show the vertical soil throw height, defined as the distance from the original soil surface to the highest point of soil particles in the front of the opener, as labeled in Fig. 11b.

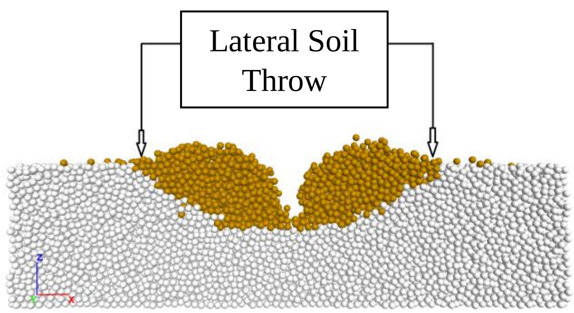

(a)

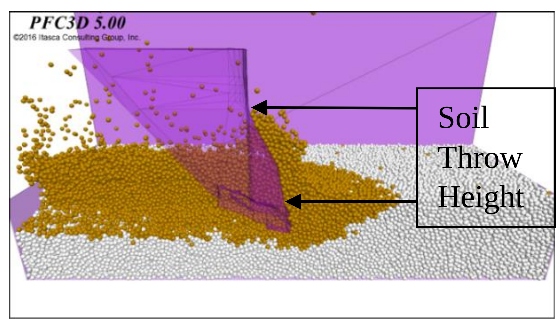

(b)

Figure 11a - Lateral soil throw distance measurement. Figure 11b - Vertical soil throw height measurement.

Model Calibration Field data of soil torque from vane shear tests was used to calibrate the model particle microproperties so that the model particles would reflect the soil from the field. For this, a virtual test using the vane shear meter was created using PFC^{3D} 5.00.23. As the shearing action of the vane shear meter acts in a circle around the vanes, walls constraining particles in the model were created as a cylindrical can with a 75 mm radius and a 200 mm height. A cap was placed on the bottom of the can to ensure that particles would not fall straight through. The diameter of the can was chosen to be significantly larger than the working diameter of the vane shear meter as to minimize the computational while ensuring no edge effects.

The particles that were generated into the can were chosen to be the same size and shape as the particles in the soil-hoe model to ensure similar functioning of the calibrated microproperties. Particle-particle and particle-wall contacts were described the same as they were in the soil-hoe model, using the linear parallel bond model (Itasca 2015) and linear model (Itasca 2015) respectively. A total of 25,000 particles were generated and allowed to settle under the influence of gravity until the average mechanical energy in the particles was below the 0.001 J threshold. After the mechanical energy criterion was achieved, particles that rested above the 100 mm level were deleted to create a level soil surface. After deletion, 16,837 particles remained in the testing system and these particles were then assigned microproperties (Table 2).

Table 2 - Soil-hoe model particle microproperties.

Property	Value
Friction coefficient (μ)	0.5
Normal stiffness (k_n), Pa	1e4
Bond normal and shear stiffness ($\bar{k}_n$), Pa	2.5e9
Viscous damping coefficient (β)	1.0
Local damping coefficient (α)	0.5
Effective modulus (E_{mod}), Pa	To be calibrated

The model vane shear meter was simplified as four vanes having the same dimensions as the vanes on the real shear meter (Fig. 12a). These vanes were represented by the built-in box wall function in PFC^{3D} of dimension 16.5 x 50 x 2 mm each. The four vanes were lowered into the particles at a slow speed (0.25 m/s) until the top of the vanes were level with the soil (Fig 12b). The vanes were rotated at a speed of 1rpm which was the same as in the field tests.

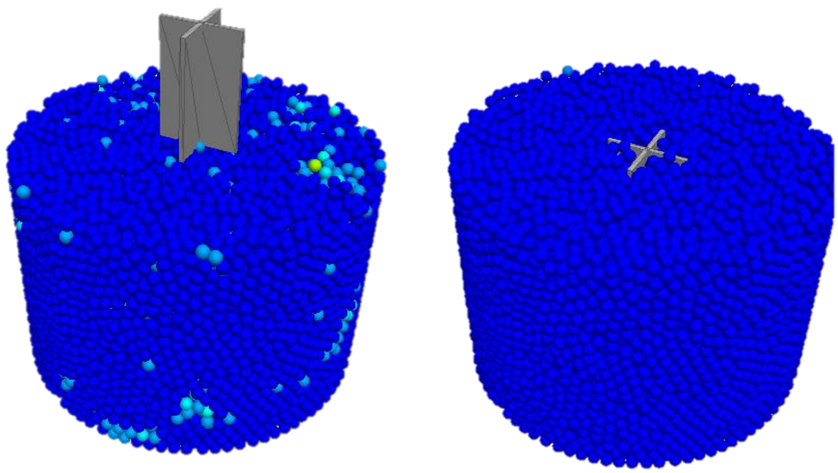

(a) (b)

Figure 12a - Generated vane shear meter. Figure 12b - Model state prior to operation.

Using the built-in *history* function in PFC^{3D}, the contact forces on each of the simulation vanes were recorded and then converted to torque. Preliminary virtual tests using the vane shear model showed that the effective modulus (E_{mod}) parameter of the linear parallel bond contact model had the most significant effect on the output torque exerted on the vanes. Therefore, E_{mod} was chosen to be the calibration parameter.

Model Validation The soil-hoe model was validated using the field soil disturbance data. The model opener was run at a working depth of 38 mm seedbed and a travel speed of 2.22 m/s to match the field testing parameters. The lateral throw distance of the particles was measured for comparison with the field data.

Model Application Using the validated soil-hoe model, the previously tested opener (single shoot spread opener) as well as three other hoe-type openers were simulated against each other to examine their cutting forces and soil disturbance characteristics. These are critical factors for designing and prototyping new soil-engaging tools. The three openers in question were a double shoot side band opener, a double shoot paired row opener, and a triple shoot opener. These openers were chosen as they had significant design differences that would be highlighted by the simulation results.

In the same method as was in the soil-hoe model development, each opener was modelled in Autodesk Inventor Professional 2016 and then imported into the soil bin simulation model. Comparisons were made with each opener operating at a travel speed of 2.22 m/s and a working depth of 38 mm. The simulation was set to record the lateral, vertical, and draft forces of the openers as well as the soil lateral throw distance and vertical throw height using the previously mentioned methods.

The double shoot side band opener is an asymmetrical opener that places seed down in a band behind the opener point and places granular fertilizer out to the side in a second band behind the opener's single wing (Figs. 13a). The opener had a 19 mm point with a 38.1 mm wing. The wing side of the opener also has a small chute that comes down behind the wing to deliver fertilizer.

The double shoot paired row opener (Figs. 13b) is a symmetrical opener that places granular fertilizer down in a band behind the opener point and places seeds out to the sides in a set of paired rows on either side of the fertilizer. The opener had a 19 mm point and a total wing width of 76.2 mm.

The triple shoot opener (Figs. 13c) is a slightly asymmetrical opener that places granular fertilizer down in a band behind the opener point, places seeds down a chute out to one side behind a wing, and places liquid fertilizer or NH_3 out to the other side of the opener behind the second wing. The seed side of the opener has a small chute that comes down behind the wing.

(a)

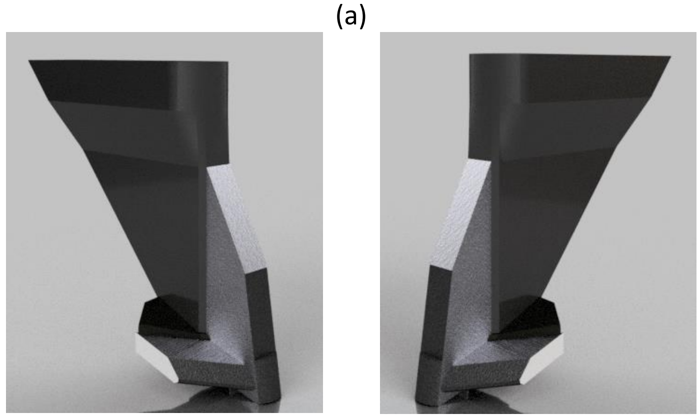

(b)

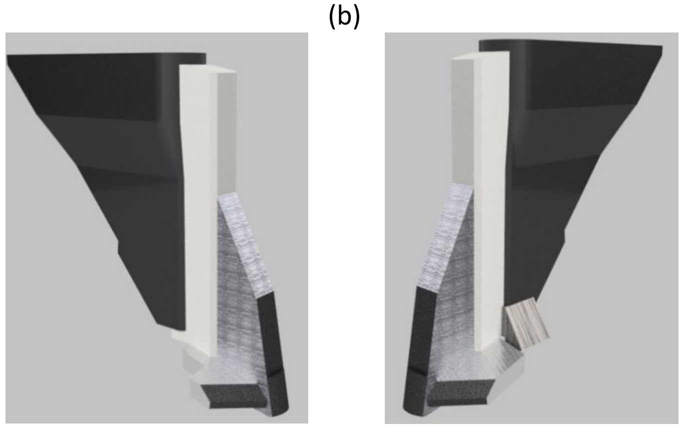

(c)

Figure 13a - Double shoot side band opener. Apteral side (left). Granular side (right). Figure 13b - Double shoot paired row opener. Figure 13c - Triple shoot opener. Liquid side (left). Seed side (right).

5 – Results and Discussion

5.1 - Results from Disc Opener

Soil Bin Test Results

Measured Soil Throw The soil used in the soil bin test had an average moisture content of 19.6% (dry basis) and the average dry bulk density of the soil was 1560 kg/m^3, which were typical for sandy loam soils. Soil throw results from the soil bin testing showed that with a tilt angle of 0°, the disc threw the soil the shortest distance, whereas the 20° tilt angle threw the soil the greatest distance (Fig. 14). The trend showed that the soil throw increased linearly as the tilt angle of the disc was increased.

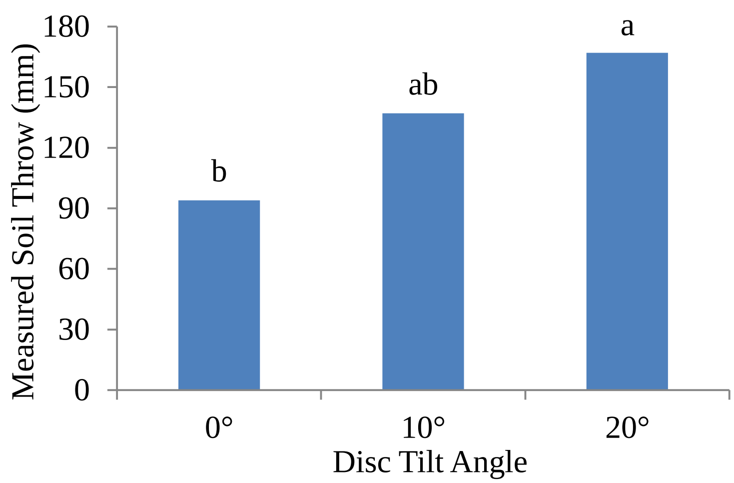

Figure 14 - Measured soil throw results; Values labelled with the same letters were not significantly different at α=0.05

Measured Soil Cutting Force Vertical force results of the tested disc showed that the 0 and 10° tilt angles resulted in similar vertical force and further increasing the tilt angle to 20° resulted in increased vertical force (Fig. 15). The draft forces for the 10 and 20° were much higher than that for the 0°. Force results of the tested disc did not show any particular trends or statistical significances due to the highly variable data. This is typical due to the non-homogeneous nature of soil. Average results over all three angles were 21 N for the vertical force and 18 N for the draft force.

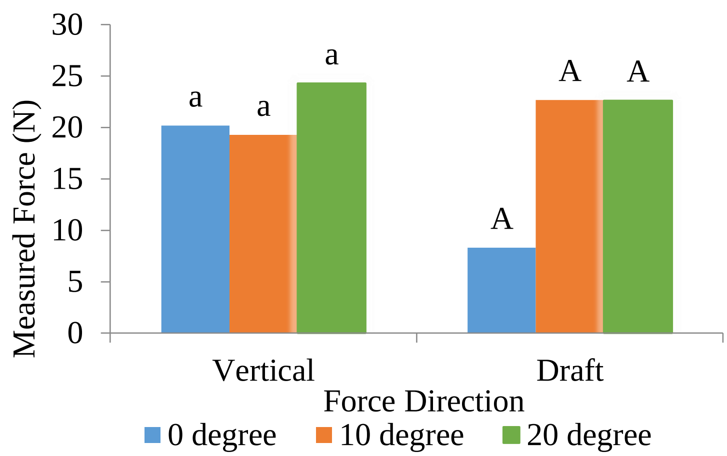

Figure 15 - Measured soil cutting force results; Values labelled with the same letters were not significantly different at α=0.05

Soil-Disc Model Validation

Comparison of Soil Throw Validation of the model was performed against the soil throw results from the physical soil bin testing. Figures 16a, 16b, and 16c show the soil displacement gradients of the 0°, 10°, and 20° vertical tilt angles respectively. The 0° tilt angle left a very tight band of disturbed soil on the right side of the furrow. The lateral soil throw distance away from the furrow increased when the tilt angle was increased to 10° and 20°.

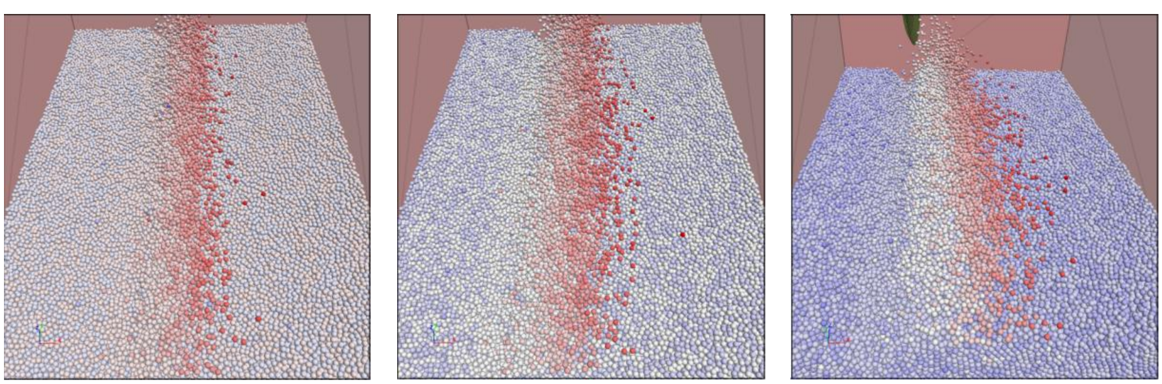

(a) (b) (c)

Figure 16a - Soil throw at 0° tilt. Figure 16b - 10° tilt. Figure 16c - 20° tilt.

Figure 17 shows the model results for the soil throw under three different tilt angles. When compared to the soil bin measurements shown in Fig. 15, the model was least accurate at the 0° tilt angle with a 20.34% relative error from the measurement with the model predicting a larger value. The model prediction at the 10 and 20° tilt angles had lower relative errors (under 10%) where the model predicted a larger throw distance at 10° and a smaller throw distance at 20°. Over all three tilt angles, the average of the absolute relative errors was 10.53%, which was considered to be low. The predicted values of soil throw also had a linear trend as the measurements. All these factors suggested that the chosen model particle microproperties accurately represented the soil used in the physical testing.

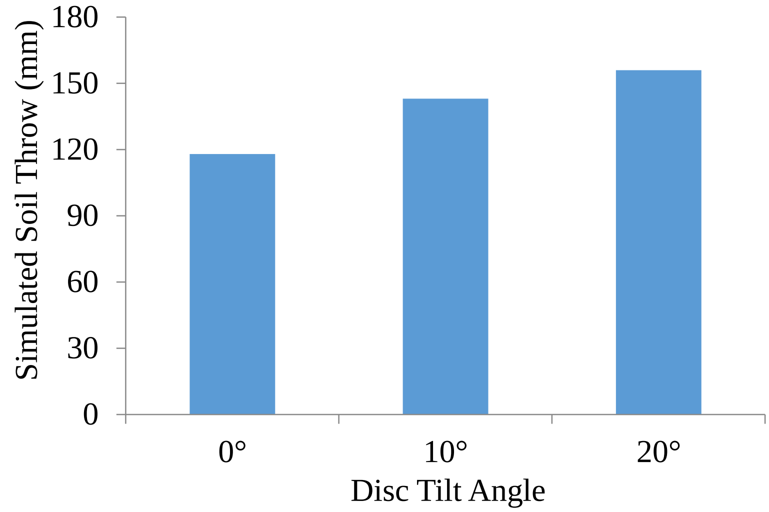

Figure 17 - Simulated soil throw results

Comparison of Soil Cutting Force Validation of the model was also performed using the draft and vertical forces through comparing the model results with the soil bin data. Model results showed a steady decrease in draft force as the tilt angle was increased (Fig. 18). In the model, at the 0° tilt angle, the average draft force of the disc was 19.1 N. This value decreased to 17.3 N at the 10° tilt angle, and further decreased to 16.2 N at the 20° tilt angle. The experimental results showed a much lower draft force at the 0° angle, and a drastic change in force at the larger angles (Fig. 15). When averaged over three angles, the simulated average draft force agreed well with the measurements with a relative error of 1.86%.

The simulated vertical force showed that an increase in the tilt angle decreased the required vertical force. The rolling action of a disc being pulled through the soil causes the disc to roll up onto the untilled soil rather than going through it. This action causes the vertical force on the tool. When the angle is changed away from vertical position, a portion of the rolling force is translated along a different axis causing a decrease in the vertical force on the disc. Results from the model showed that the vertical force of the disc was highest at the 0° angle with an average value of 13.71 N. Each consecutive increase in the tilt angle caused a decrease in the vertical force. At 20°, the vertical force was reduced by 38.6%. The vertical forces measured in the soil bin did not have any particular trend. The measured forces were greater than the simulated forces at all tilt angles. Over all three angles the simulated average vertical forces had an error of 50.7% relative to the measurements. The high vertical force relative error was due to high levels of variance seen in soil bin results.

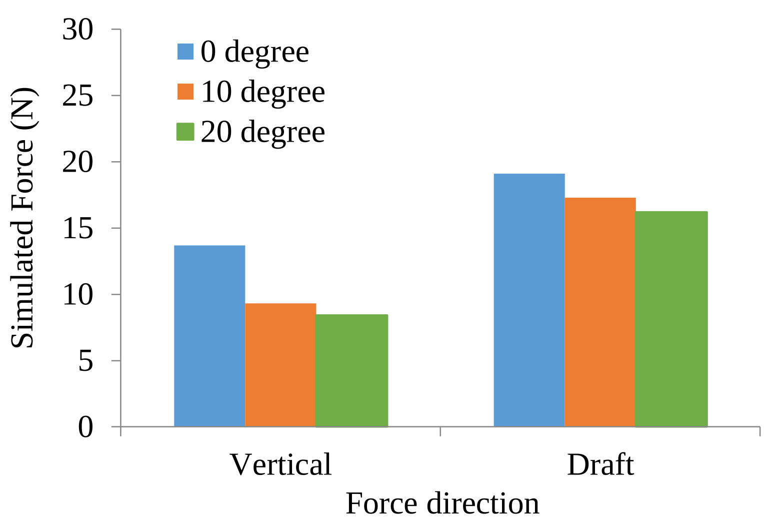

Figure 18 - Simulated force results

Soil-Disc Model Applications

Effects of Gang Angle on Forces After being validated, the soil-disc model was used to examine the effects of gang angle on the draft, vertical, and lateral forces of the disc under a constant travel speed and working depth. The simulated force-time curves are presented to demonstrate the dynamic regime of soil-disc interaction when the gang angle of the disc was increased from 0° up to 30° at 5° intervals. For all three forces, the force-time curves were more fluctuating at an increased gang angle. This implied that soil particles were more dynamic under the impact of the disc working at a larger gang angle. It was interesting to find that the magnitude of the curve fluctuation was different among the three forces. Under the same gang angle, the lateral force curves were the smoothest, whereas the vertical force curves showed the most fluctuation, leaving the draft force curves as the intermediate. These phenomena demonstrated that the disc induced the most particle dynamic forces in the vertical direction and the least in the lateral direction. The information will have important implication for the design of the disc opener assembly and the seeder frame in terms of wear and strength.

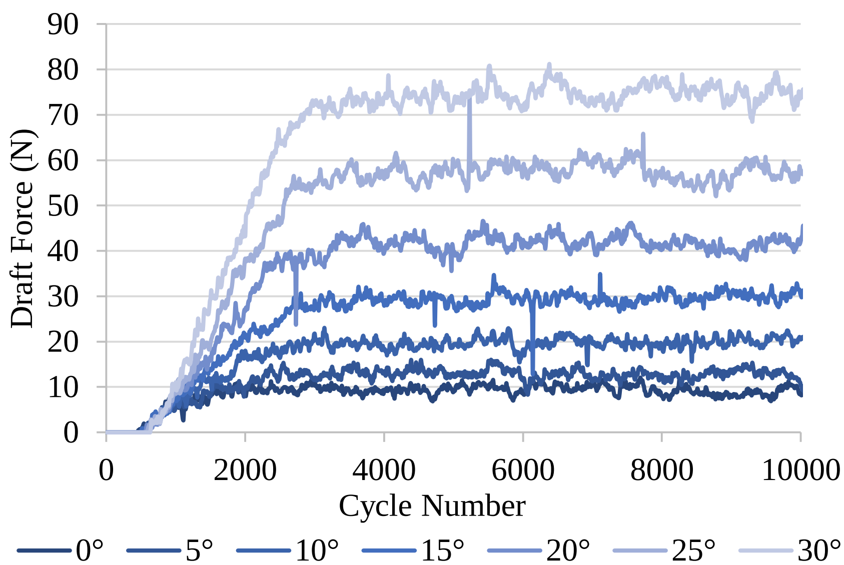

(a)

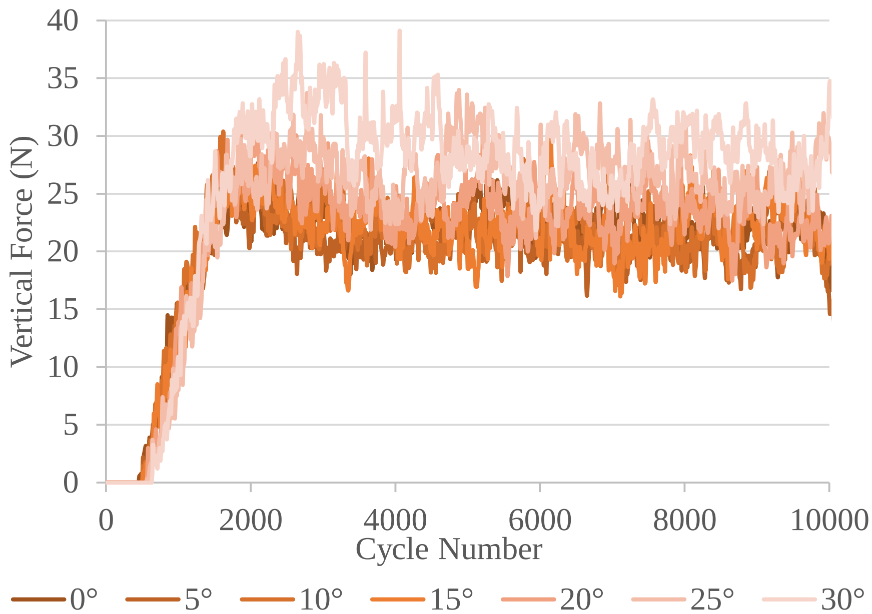

(b)

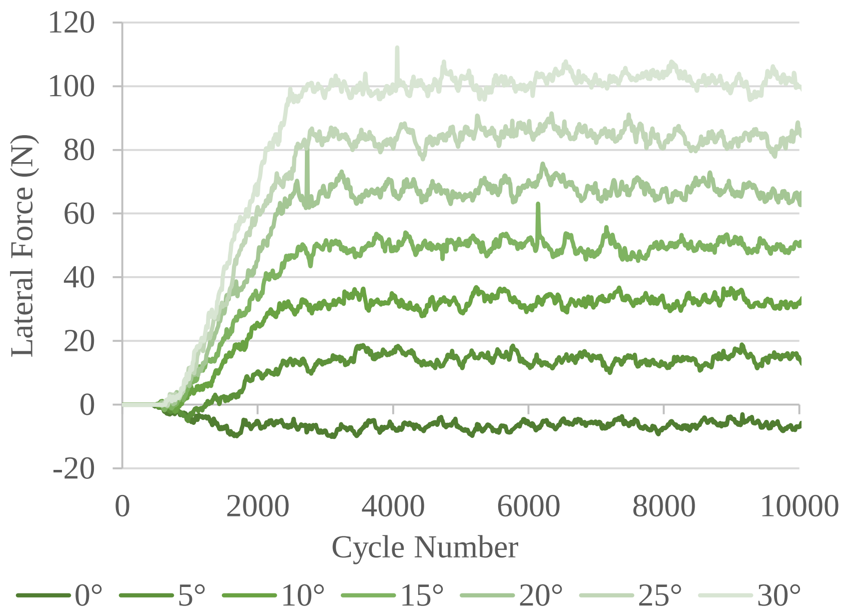

(c)

Figure 19a - Simulation results of draft force with time. Figure 19b - Simulation results of vertical force with time. Figure 19c - Simulation results of lateral force with time.

As the gang angle was increased the resultant average draft force increased from 9.38 N at 0° up to 74.67 at 30° (Fig. 20). The relationship between the average draft force and the gang angle fitted a polynomial equation with a coefficient of determination (R^2) of 1.00. The lateral force of the disc increased linearly from -6.43 N up to 101.64 N, and the linear regression equation had an R^2 of 1.00. While the draft and lateral forces had significant changes as the gang angle was changed, the vertical force changed only slightly. At 0°, the vertical force was 22.38 N. At 10°, the force decreased to 21.25N, followed by a steady increase up to 28.39N at 30°. This trend was also represented by a polynomial equation (R^2 = 0.98). These regression equations provide a clear picture of how each force is affected by the gang angle, which is important guiding information for the setup of the disc angle in practice. The results seen from the simulation testing of effects of gang angle on opener draft force are in line with those seen by Nalavade et al. (2010). In this study it was seen that both powered and free rolling disc openers saw increases in draft and vertical forces as the gang angle was increased.

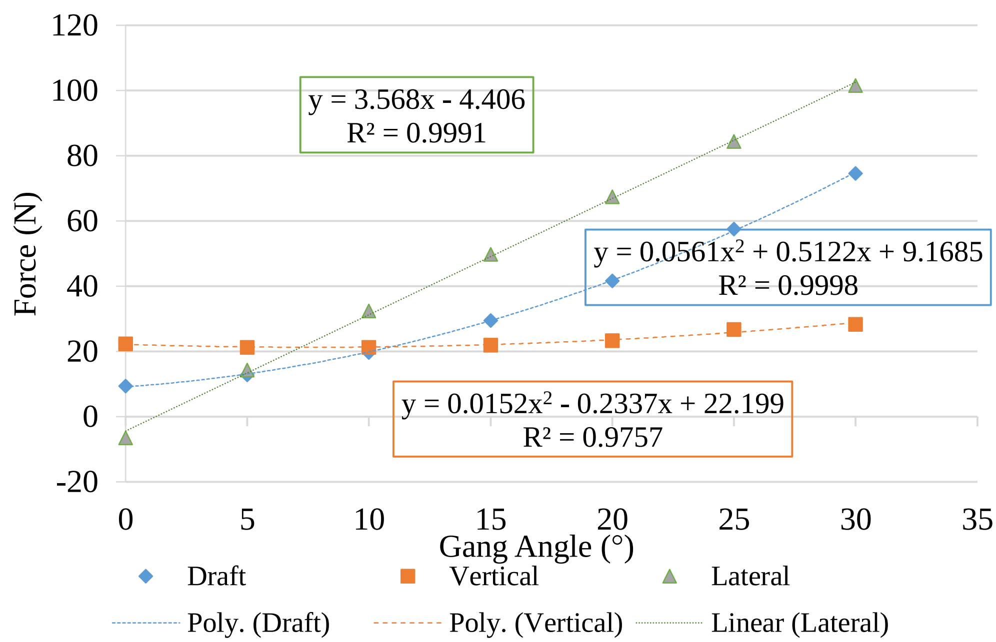

Figure 20 - Simulation results of force against gang angle

Effects of Working Depth on the Forces The effect of working depth was examined in the validated model over a depth range of 12.5 mm up to 75.0 mm in 12.5 mm increments with a constant gang angle of 10°. Similar to what was observed when changing the gang angle, the force-time curves seemed to be more fluctuating for the vertical force, followed by the draft force, and then lateral force (Fig. 21a, Fig. 21b, and Fig. 21c). The observations indicated that soil particles behaved more dynamically at the higher depths, as demonstrated by the more fluctuating curve at greater working depths.

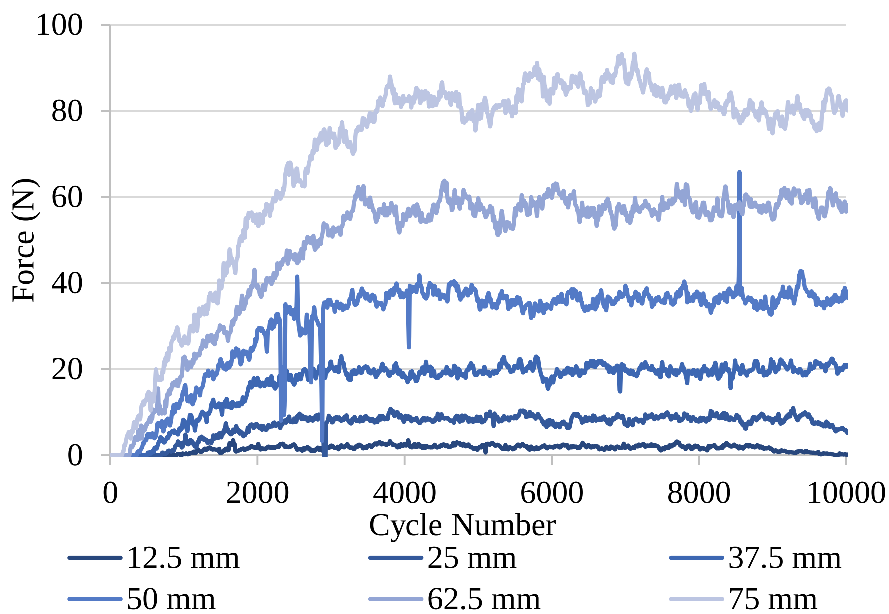

(a)

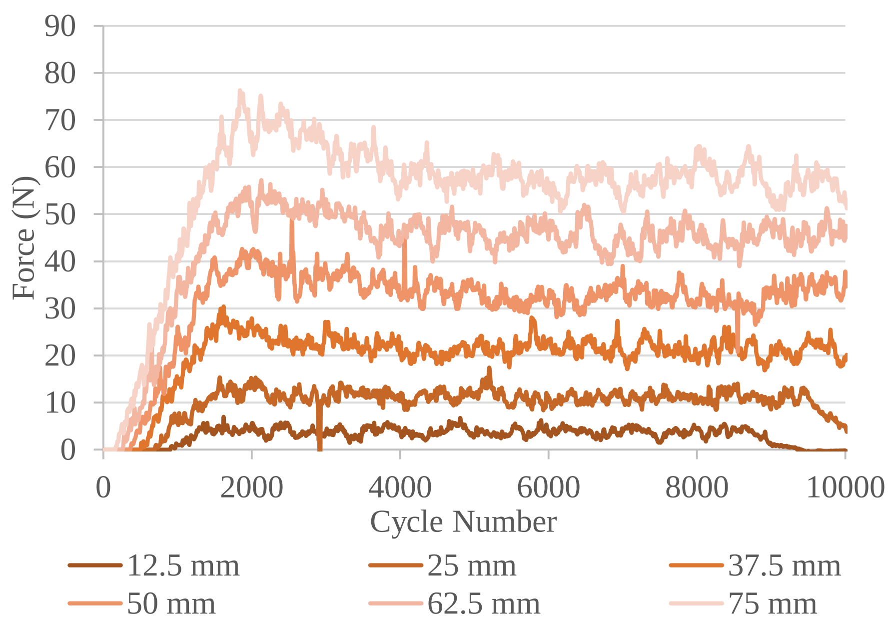

(b)

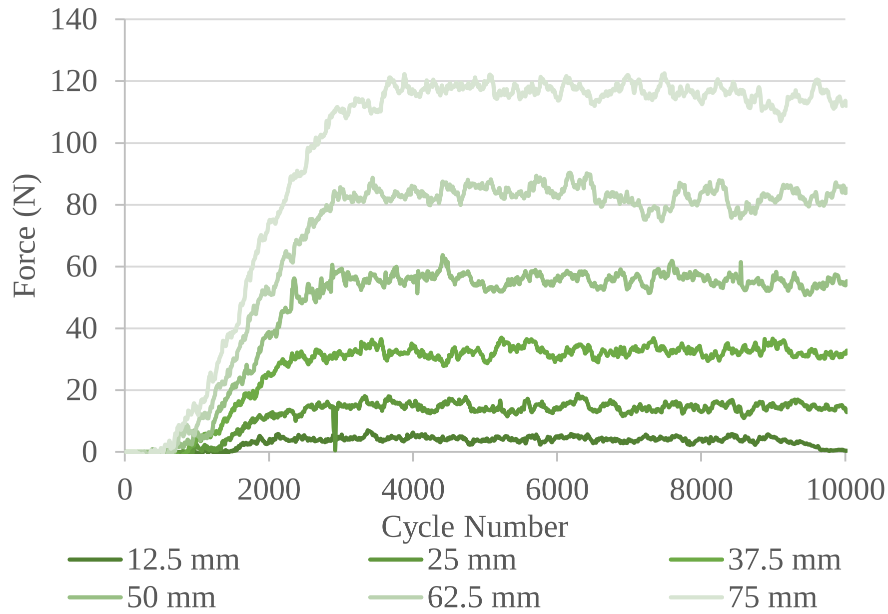

(c)

Figure 21a - Simulated results of draft force against time. Figure 21b - Simulated results of vertical force against time. Figure 21c - Simulated results of lateral force against time.

The average forces in all directions had an increasing trend as the working depth of the disc increased (Fig. 22). Draft forces increased from 1.75 N up to 82.87 N as the depth was increased from 12.5 to 75 mm. Over this depth range, lateral forces increased as well from 3.84 N to 116.49 N. Both forces and their relationships with working depth could be described by a polynomial equation with an R^2 of 1.00. Unlike the insignificant effect of gang angle on the vertical force, working depth had a significant effect on the vertical force. The vertical force linearly increased from 3.13 N to 57.40 N over the depth range studied herein. The high R^2 values in all cases indicated that these regression equations described the simulated draft, vertical, and lateral forces well, and can be used to predict forces of the disc under different working depths.

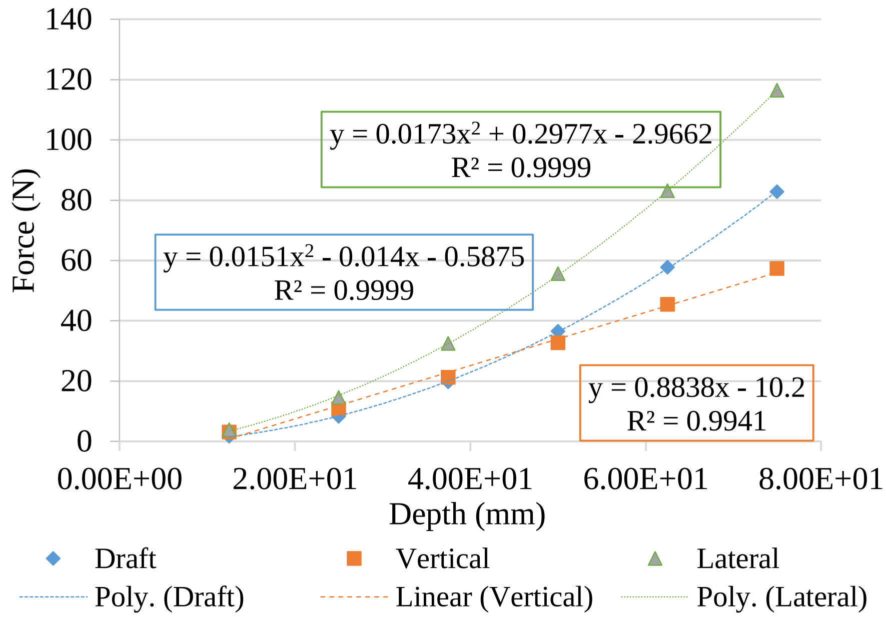

Figure 22 - Simulated results of force against working depth.

5.2 - Results from Hoe Opener

Field Test Results

Results of the field soil conditions are summarized in Table 3. Soil across the field was quite uniform at the time of seeding, in terms of bulk density. The average dry bulk density was 982 kg/m^3, which was typical for the surface layer of a clay soil. The moisture content was also reasonably uniform, which was unexpected, as the measured locations were in low and high areas of the field. The average moisture content was 25.0%, meaning the field was quite dry for a clay soil. This explained the uniform moisture content, and the observation that the soil surface penetration resistance and soil shear torque showed little change from the low to high area of the field. The dry soil condition of the field suppressed the effect of other soil properties such as soil cohesion and friction. Surface residue cover also had low variability across different areas of the field, and the average residue cover was 17.4%. This moderate residue cover would not have any impact on the field measurements of soil properties. Soil throw results from the air drill varied slightly with the field condition, and the average value over all areas was 212.4 mm. This value was used for the model validation discussed later in the thesis.

Table 3 - Summary of field test results.

Soil Condition (Elevation)	Dry Bulk Density (Kg/M^{3})	Soil Moisture Content (d.b. %)	Resistance (Kg)	Torque (Nm)	Residue Coverage (%)	Soil Throw Distance (mm)
Low	978.2	24.9	7.10	2.22	17.16	198.6
Mid	999.2	25.8	7.36	2.21	16.24	214.7
High	968.5	24.4	6.96	2.00	18.68	223.9
Average	**982.0**	**25.0**	**7.14**	**2.14**	**17.36**	**212.4**

Soil-Hoe Model Calibration

Calibration of the soil-hoe model was performed to match the results from the virtual vane shear test and the measurements using the vane shear meter in the field tests. As mentioned previously, effective modulus (E_{mod}) was chosen as the microproperty to be calibrated. In the calibration, 15 values of E_{mod} were chosen within the range 2e5 and 1e8 Pa. Outputs of contact forces between particles and the vanes of the model vane shear meter from the simulation are shown in Fig. 23. The forces reached their maximum values at the very beginning of the simulation, meaning that soil particles failed as soon as the model vane shear meter was rotated. As the rotation continued, the contact forces decreased close to a near zero value.

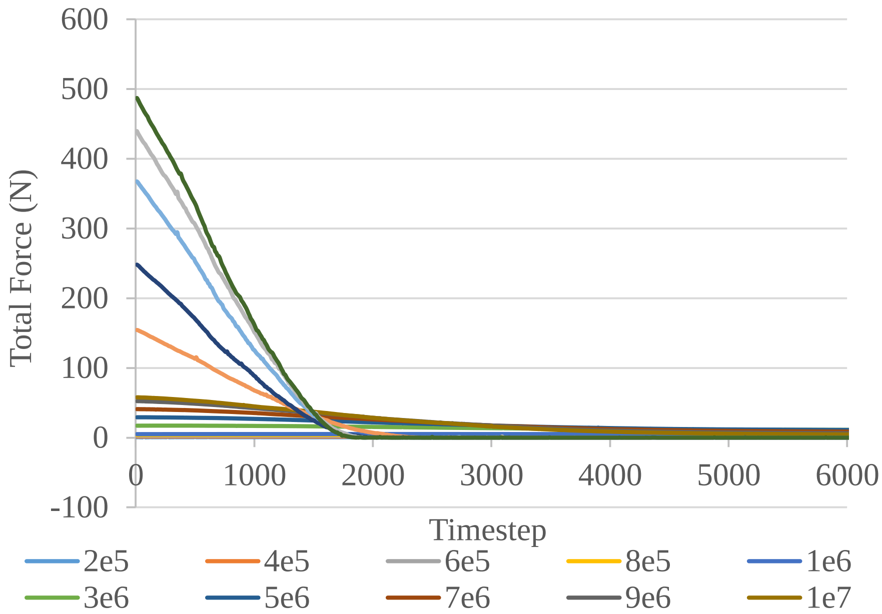

Figure 23 - Simulated results of force against time.

These results did not show a typical shear strength curve one would have expected to see where the force gradually increases up to the yield point and then rapidly decreases back to a free-spinning load. However, when the model was tested at extremely low speeds (<1/1000th) of the actual operation speed of 1 rpm the typical yield strength curve was noted. As there was no change in results between the actual speed model and low speed model, the actual speed model was chosen for running the tests to reduce computation time.

The differences between the typical shear curve and the simulated curve were due to a couple of factors. In the real vane shear meter there is a spring in the head dial and a small steel rod, that are able to absorb some of the applied torque to build up a reading before reaching the soil failure strength. In the simulation model however, these parts do not exist to slowly build up an application force during the application of torsion. Additionally, within the simulation model, the walls that made up the vanes were considered infinitely strong materials that would not deform under loading, and the rotational speed was applied by an infinitely strong motor that is able to reach any given velocity instantaneously. This caused an instant soil yield point in the output data at the 1 rpm rotational speed.

To match the torque measured in the field tests, the total contact force between particles and a vane was converted to total torque. Assuming the total contact force to be a concentrated force acting in the normal direction at the center of the vane, the torque was determined by multiplying the contact force and the distance from the center of the vane and the center of the rotation of the model vane shear meter. The total torques simulated with different input E_{mod} are shown in Fig. 24. A higher particle E_{mod} produced a higher total torque. Their relationship can be described using the following linear regression equation:

$$E_{mod} = 25{,}625{,}151.74(T) - 671{,}227.94$$

where E_{mod} = effective modulus of particle (Pa) and T = total torque (Nm). The coefficient of determination (R^2) was 1.00.

Using this equation and given the average of field measured torque, 2.14 Nm, an E_{mod} of 5.692e7 Pa produced the same torque. Thus, the value of 5.692e7 Pa was the calibrated E_{mod} value for the particles to represent the field soil.

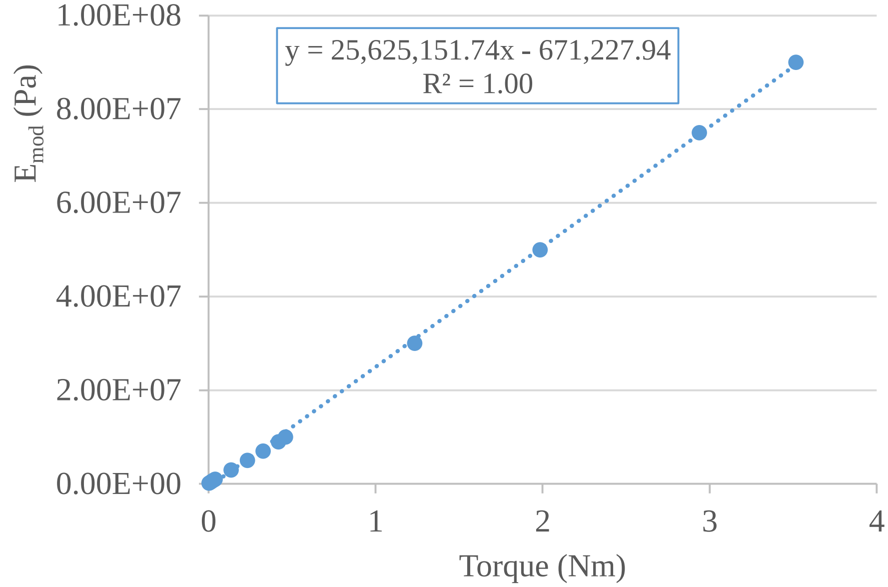

Figure 24 - Calibration curve of E_{mod} against torque.

Soil-Hoe Model Validation

Validation of the soil-hoe model was performed against the soil throw data of the hoe openers tested in the field. In the simulation, the single shoot spread opener was set at a working depth of 38 mm and a travel speed of 2.22 m/s. These operational parameters were the same as the field tests. As the model opener advanced in the model soil bin, particles were displaced and flowed around the opener. The simulation model saves an image of any view created as a movie view every 100th cycle which can then be stitched together to create a video of the view. Figure 25 shows images saved from four different views of the model during operation to visually observe the soil flow dynamics around the opener.

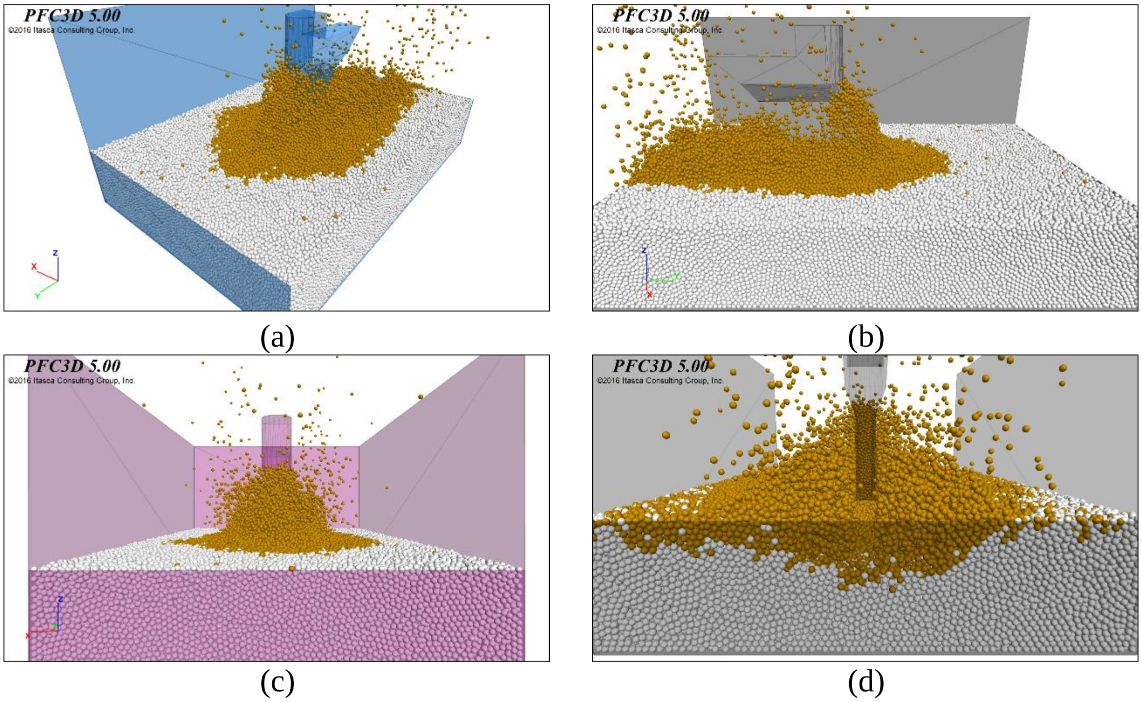

Figure 25a - Isometric operation view. Figure 25b - Side operation view. Figure 25c - Front operation view. Figure 25d - Behind operation view.

Using the calibrated E_{mod} (5.692e7 Pa) as the soil-hoe model input, the average soil throw distance simulated for the tested opener (the single shoot spread opener) was 243.92 mm. Comparing this simulated soil throw to the field data (212.4 mm) gave a relative error of 14.8%. This shows a good correlation between the simulation and measurement.

Soil-Hoe Model Application

Prediction of Soil Cutting Force Draft force is typically considered to be the most critical of the forces for soil-engagement tools as it is the amount of force needed to pull the tool through the soil. Smaller draft force requirements are considered to be better as this means that either a smaller horsepower tractor will be required to pull a toolset, or a larger number of tools can be pulled without the need for a larger tractor. Simulated draft forces for the four different openers are shown in Fig. 26. The draft force varied among the openers that had different tool geometry. It is expected that the major geometries, such as the point and wings of opener, contributes significantly to the force. However minor features, such as chutes and boots, can also make a difference in the draft requirements of an opener. The draft forces of these openers can be explained based solely on the geometry of the openers. The double shoot side band opener had the lowest draft force (287.16 N) of the four tested openers. A significant increase in draft force was seen for the other three openers. This could be explained by the fact that the side band opener only had a single wing whereas the other three openers had two wings each. The second lowest draft force was observed for the triple shoot opener which had a chute behind one wing and a slightly smaller wing on the opposite side. The double shoot paired row opener had a slightly higher draft requirement than the triple shoot opener. This opener had two full size wings and a seed depositing cup behind the wings that would account for the slight increase in draft requirement. Finally, the single shoot spread opener had the largest draft requirement due to the higher total working width of 101.6 mm whereas the other two double wing openers were only 76.2 mm wide.

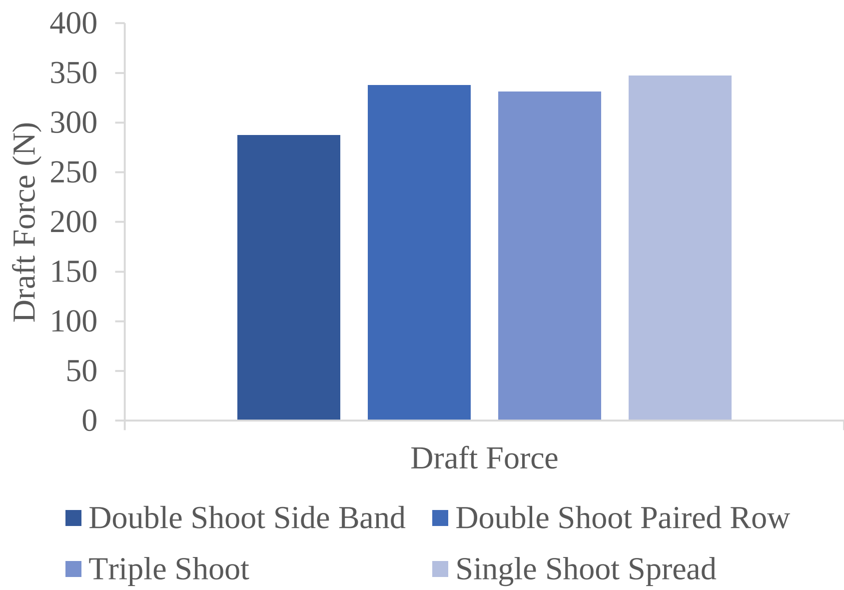

Figure 26 - Comparison of opener draft forces

The vertical force measures the amount of force required to push the opener into the soil and maintain the desired operation depth. This force contributes to the amount of hydraulic power or weight of the implement required to ensure that the opener will not push itself out of the soil or will not pull the machine down further into the soil. Similar to the design factors that influence the draft force on an opener, certain design choices can influence the amount of floatation that a soil-engagement tool will have. The openers were designed with a point rake angle close to vertical (84°) for implementing opener “float” at the desired operation depth. Results of simulated vertical forces ranged from 38.21 N up to 87.19 N (Fig. 27). As with the draft force, the double shoot side band opener had the lowest vertical force of all the tested openers. This was due to having only one wing to pull the opener down into the soil. The triple shoot opener had the next lowest vertical force load at 46.41 N which was due to the additional second wing. The double shoot paired row ranked third at 55.71 N due to location of the seed depositing cup behind the wings that was slightly higher than the top of the wing, meaning that the cup acted as part of the soil-engagement area. Finally, as with the draft force, the single shoot spread opener had the largest vertical force by a significant amount due to the much larger working width than the other openers and the tilted up wings, which increased the furrow area that is used to spread the seed and fertilizer.

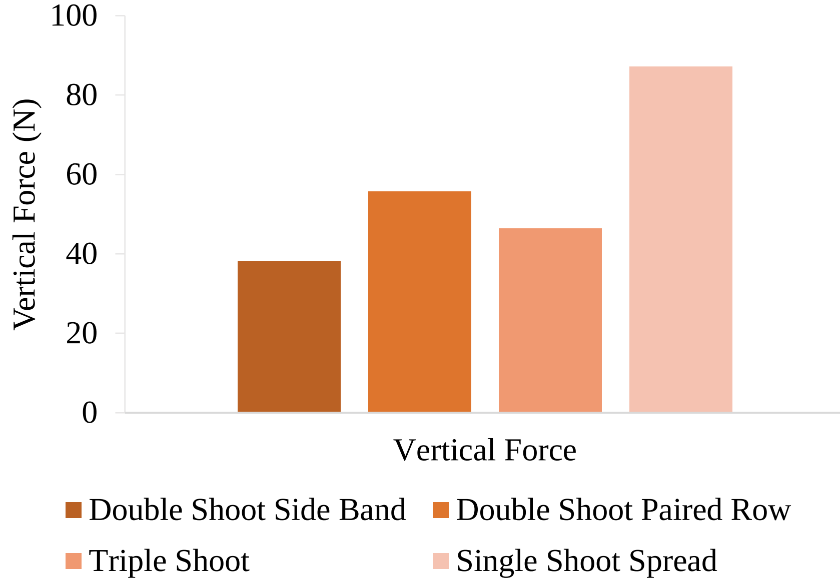

Figure 27 - Comparison of opener vertical forces.

Lateral force is not typically considered to be a critical force while designing prototype openers; however, this force has an effect upon the performance of the opener and the life of the implement. Generally, the shanks of openers are designed to take the applied force from the opener and transfer it up to the frame of the machine. Side loads (lateral forces) can cause the shanks to twist and unevenly allocate stresses on locations that are not designed to handle stress. The double shoot side band opener had extremely high lateral force (86.55 N) due to its asymmetrical geometry (Fig. 28). The lateral force of the triple shoot opener was only 25% of the double shoot side band opener, and those of the other two openers were negligible.

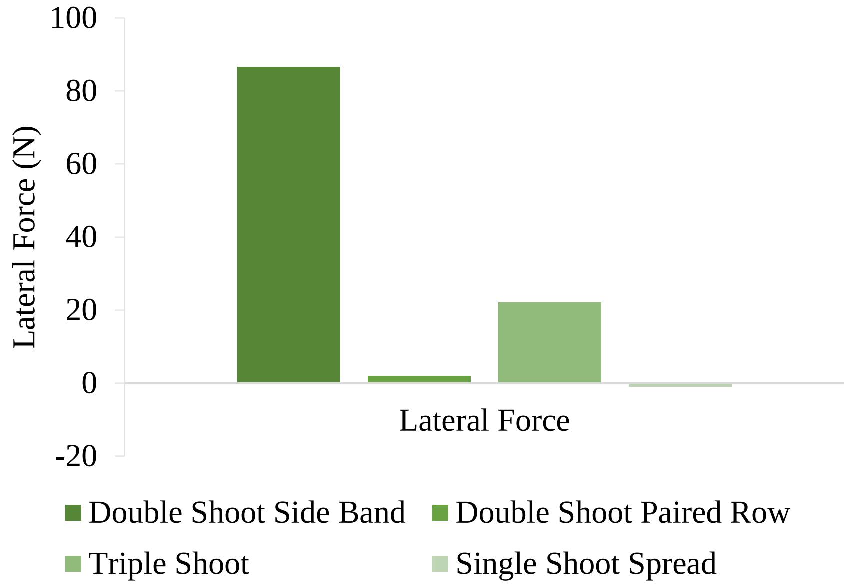

Figure 28 - Comparison of opener lateral forces.

To use PFC^{3D} simulation for prototyping new openers, the strength of the program does not necessarily lay in the direct output values. While it is a good design practice to know the approximate tractor horsepower requirement for a set of openers, it is not the most pertinent information during the design phase. Taking the results of all forces and charting them as a percentage of the total load, as seen in Fig. 29, shows where the proposed prototype could have issues. A primary concern while designing new prototype openers is where the opener is going to wear down. The forces of the soil on the opener is what causes the openers to wear down as they correlate to the amount of contact with the opener. Further refinement of the simulation output would allow us not just to estimate the lateral, vertical, and draft loads on the entire opener, but to also show those forces acting on the wings and points separately, which would allow designers to determine where the prototype will need stronger materials. All four tested openers show the draft section of Fig. 29 to be the most significant force which would suggest that the openers need to be protected the most from the front. In reality, the openers have a hardened steel point which has carbides brazed on for additional protection. The green segment of Fig. 29 shows that the double shoot side band opener would require additional attention towards shank design to ensure that the twisting action of the opener will not cause excess damage.

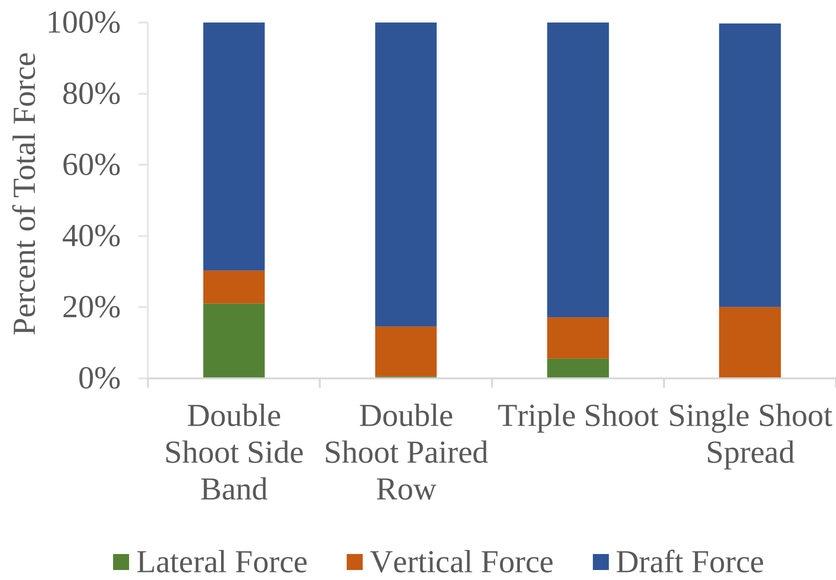

Figure 29 - Force component percent comparison.

Prediction of Soil Throw Results for the lateral soil throw distance (Fig. 30) were shown as total soil throw, which was the sum of the soil throws on two sides of opener, as well as the soil throw on separate sides of opener for the two asymmetric openers. The soil throw results showed a nearly identical trend to the draft force results in terms of how the openers ranked against each other for performance. The double shoot side band opener showed the smallest soil throw which is due to the presence of a single wing to disturb soil to the side. The smaller green bars in Fig. 30 show the difference in the throw to each side of the opener for the two asymmetrical openers. The double shoot side band threw nearly double the distance to the wing side as it did to the apteral side of the opener. The second asymmetrical opener, the triple shoot, had the second lowest soil throw of the four openers at 227.4 mm. This opener threw soil significantly further than the double shoot side band however threw only slightly less than the two other double winged openers. This difference comes from the differences in geometry for liquid and granular fertilizer chutes. Liquid fertilizer is deposited into the soil through a small (<19 mm) tube whereas the granular fertilizer requires a large chute to accommodate the solid product. The liquid tube is therefore able to be hidden entirely behind the wing allowing it to have no effect on the soil disturbance, whereas the granular chute protrudes past the side of the boot and above the wing contributing to the soil disturbance significantly. Finally, both the single shoot spread and the double shoot paired row openers had very similar soil disturbance values of 243.9 mm and 245.9 mm, respectively. Despite the single shoot spread opener having larger wings than the double shoot paired row opener, it threw slightly less soil laterally than the smaller opener. This could be explained by the seed depositing cup that rested behind the wings on the double shoot paired row opener as it caused soil to be lifted further up and allowed it to travel further out; whereas the single shoot spread opener was made to slice through the soil and therefore dropped most of the disturbed soil back into the furrow.

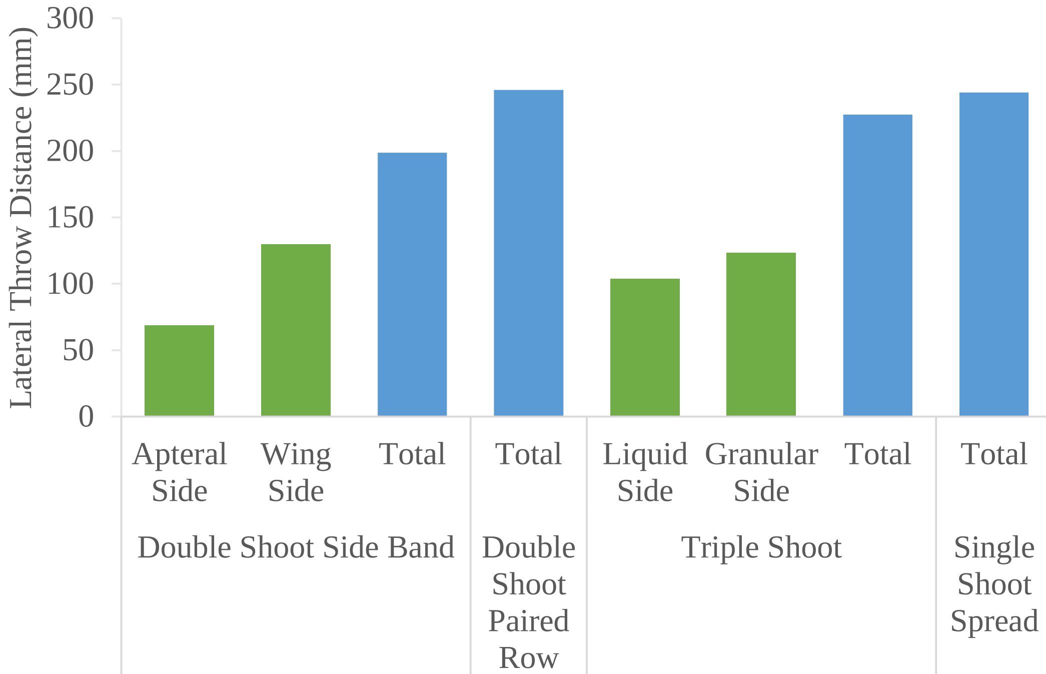

Figure 30 - Simulated soil throw results.

Figure 31 shows a view of the soil bin looking down on the furrow after the opener has passed through the bin for each of the tested openers. All particles begin the simulation with a white color, and changed to orange once they had been displaced more than 5 mm. It became easier to see the asymmetrical soil disturbance patterns (Fig. 31a, Fig. 31c) as well as the symmetrical ones (Fig. 31b, Fig. 31d).

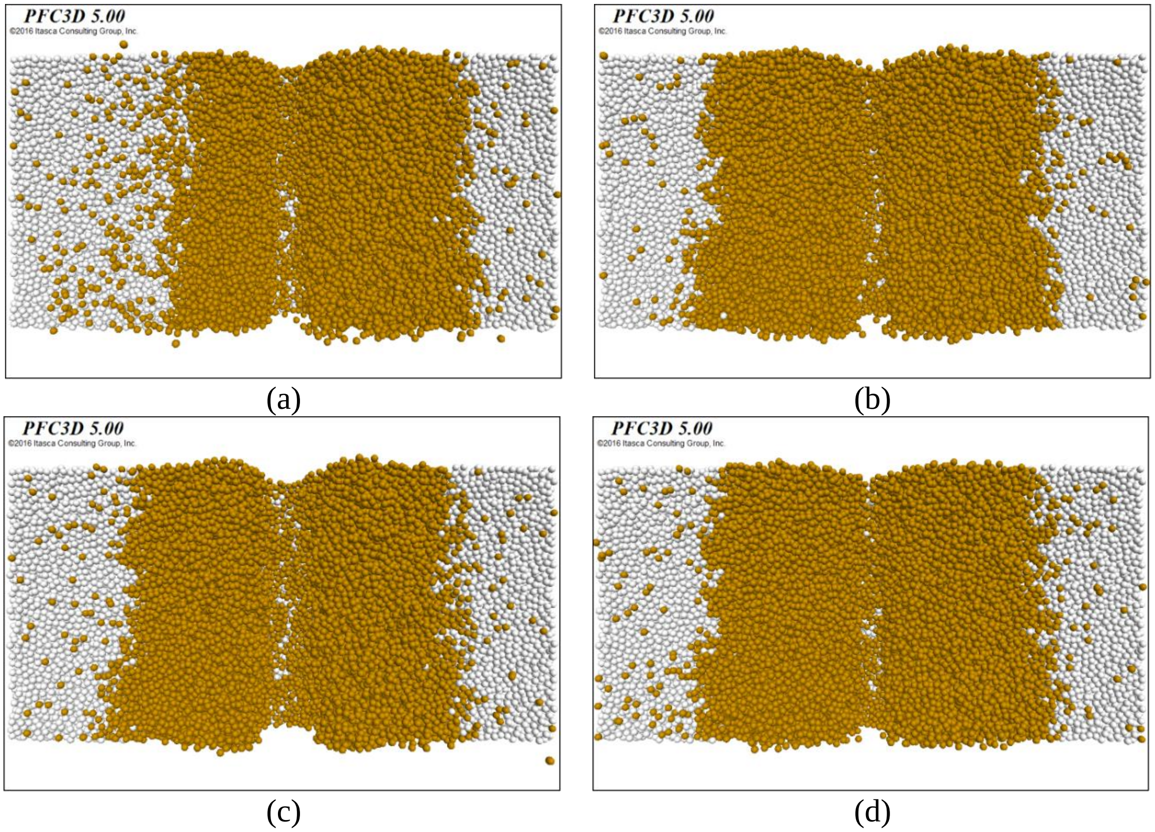

Figure 31a - Double shoot side band soil throw. Figure 31b - Double shoot paired row soil throw. Figure 31c - Triple shoot soil throw. Figure 31d - Single shoot spread soil throw.

Different soil disturbance patterns resulting from the four openers can also be seen from the furrow profile cross-sections taken from the soil model after the passage of the model opener (Fig. 32). The two openers with the asymmetrical patterns should be noted. The double shoot side band opener showed the most asymmetrical throw pattern of all the test openers due to only having a wing on one side. This is seen in the image as there is a much larger amount of disturbed (orange) particles to the left of the furrow (Fig. 32a). The triple shoot opener produced a slightly asymmetrical furrow profile (Fig. 32c), and the other two openers had symmetric profiles.

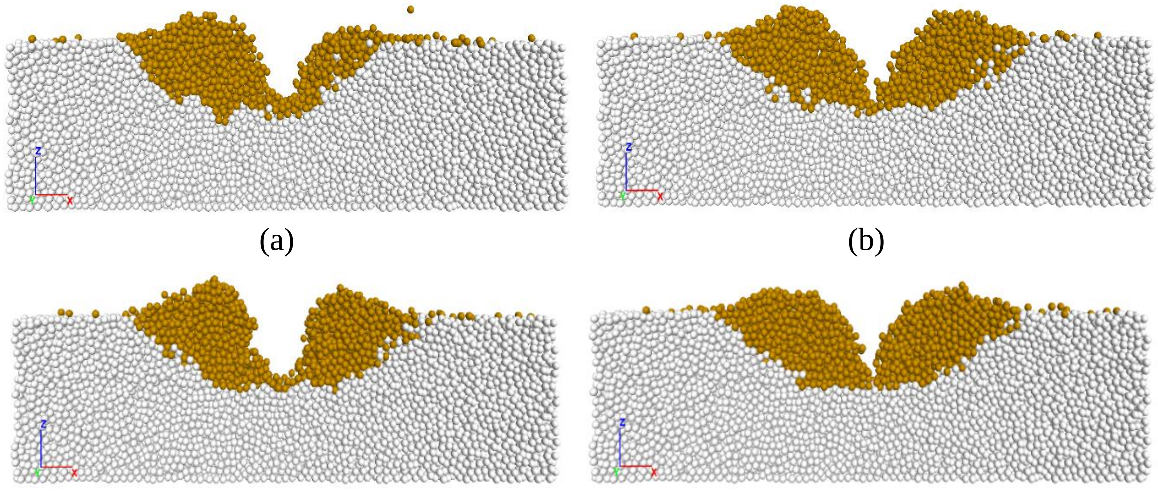

(a) (b) (c) (d)

Figure 32a - Double shoot side band furrow profile. Figure 32b - Double shoot paired row furrow profile. Figure 32c - Triple shoot furrow profile. Figure 32d - Single shoot spread furrow profile.

Prediction of Soil Vertical Throw Height As soil rides up the hardened steel point it will eventually come in contact with the mild steel boot the higher it rides up. This can lead to premature wear on the openers and is considered a critical factor during the design stage. The double shoot paired row opener kept the soil the lowest, having the soil only reach the top of the point, which was 95.5 mm (Fig. 33) above the soil surface. The single shoot spread opener allowed soil to travel 114.3 mm up the opener, placing the soil slightly onto the mild steel boot. The double shoot side band opener allowed approximately 10 mm more travel up the boot with a total distance of 124.46 mm, and the triple shoot opener fared the worst, allowing 140.46 mm of travel above the soil surface.

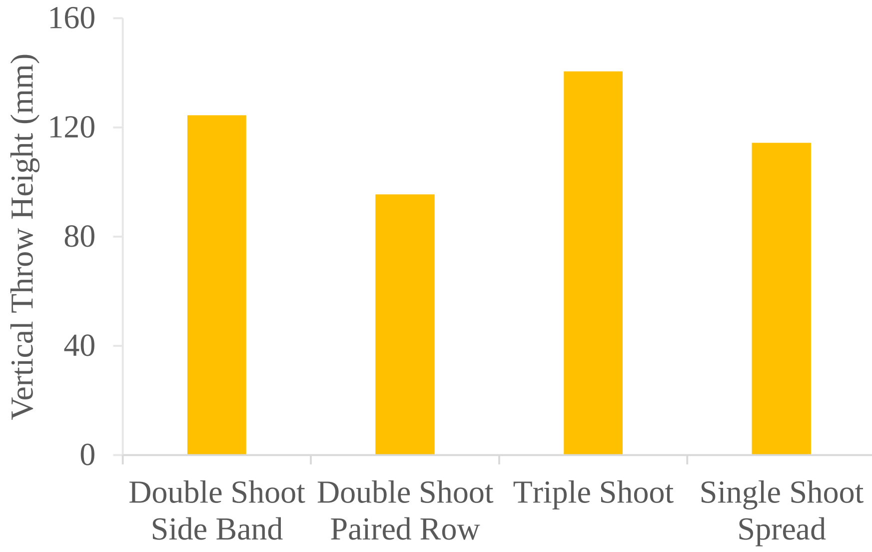

Figure 33 - Comparison of simulated vertical throw height.

The cross-sectional view of the running model also allows the user to observe how the soil particles react below the soil surface level, which is impossible to observe in field operation. Figure 34 shows this cross-sectional view for each of the four openers. While all four openers used a vertical point that was designed to fracture the soil far ahead of the working tip of the point, they had slightly different amounts of disturbed particles. The ability to see the subsurface engagement effects of the openers becomes increasingly useful as different types of opener points are designed and tested using the model.

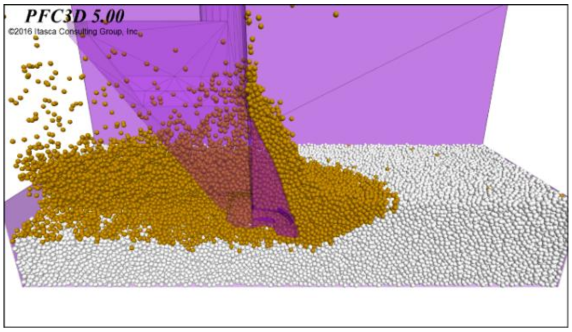

(a)

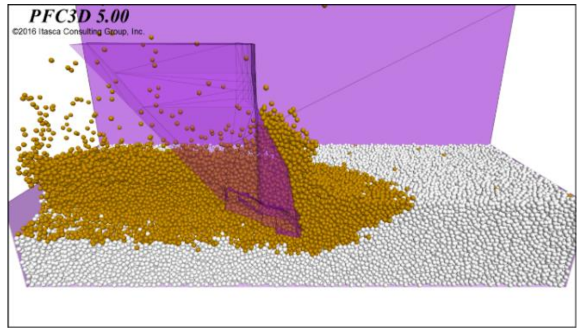

(b)

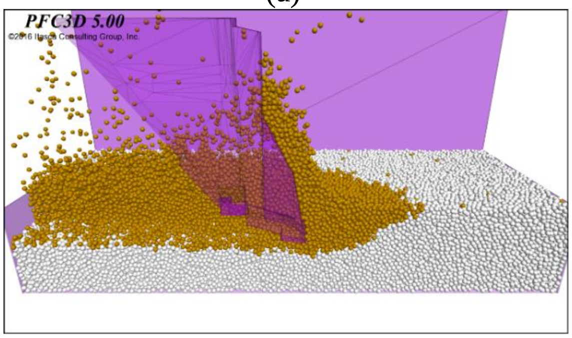

(c)

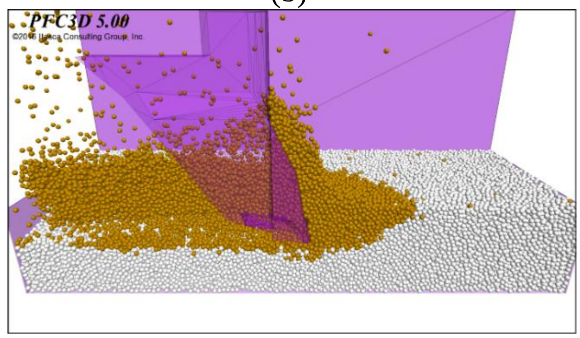

(d)

Figure 34a - Double shoot side band cross-section. Figure 34b - Double shoot paired row cross-section. Figure 34c - Triple shoot cross-section. Figure 34d - Single shoot spread cross-section.

6 – Conclusions

In this study, a soil-disc model and a soil-hoe model were developed to simulate soil and tool interaction using PFC^{3D}. The models were calibrated and validated using laboratory or field measurements. The validated models were then used to predict soil dynamics properties (soil disturbance and cutting forces). The following conclusions were drawn:

1. Based on the soil bin experimental results, smaller tilt angles should be used for the disc opener to minimize the soil throw. Tilt angle did not significantly affect the vertical force and draft force of the disc.
2. The soil-disc model results further demonstrated that smaller tilt angles could reduce the soil throw resulting from the disc. However, the model results also revealed that smaller tilt angle may increase the draft and vertical forces of the disc, which is not desired.
3. The soil-disc model results agreed well with the soil bin measurements, in terms of the average soil throw and draft force of the disc. The model was unable to accurately estimate the vertical force of the disc.
4. Further application of the soil-disc model to examine effects of gang angle and working depth of the disc showed that the draft, lateral, and vertical forces increased in either a polynomial or a linear fashion, when the gang angle was varied from 0 to 30^{o}, or when the working depth was varied from 12.5 to 75 mm.
5. In calibration of particle microproperties for the soil-hoe model, the relationship between the vane shear model output torque and the particle effective modulus was found to be highly linear. The linear equation generated a value of 5.692e7 Pa that best matched the torque measured in the field with a clay soil.

6. The soil-hoe model reasonably represented the observed interactive behavior of the hoe opener with the clay soil, in terms of soil throw. The relative error of 14.8% between field and model results show that while the model can represent soil-hoe interactions, further testing is required.
7. The further applications of the soil-hoe model to compare different openers revealed that opener geometry significantly affected the soil cutting forces and disturbance. The effect of wing geometry on lateral and vertical force, as well as soil disturbance were the most pronounced.

The soil-disc and soil-hoe models are capable of simulating effects of different tool geometrical and operational parameters. This demonstrated that the models will be very useful in designing and prototyping soil-engaging tools, saving the cost for making prototypes and actual tests. However, the models were calibrated and validated against only one soil type. Cautions should be taken when using these models for other soil types and conditions.

References

Abo-Elnor, M., R. Hamilton and J.T. Boyle. 2004. Simulation of soil-blade interaction for sandy soil using advanced 3D finite element analysis. *Soil & Tillage Research* 75(1): 61-73.

Alexandratos N and Bruinsma J. 2012. World agriculture towards 2030/2050. Food and Agriculture Organization [online]. Available from: http://www.fao.org/docrep. Accessed 2016 April 7.

ASABE Standards. 2012. "S358.2, Moisture measurement - Forages". *American Society of Agricultural and Biological Engineers*. St. Joseph, MI: ASABE.

Baker, C.J., K.E. Saxton and W.R. Ritchie. 1996. *No-tillage Seeding: Science and Practice*. Cab International.

Chaudhuri, D., 2001. Performance evaluation of various types of furrow openers on seed drills - A review. *Journal of Agricultural Engineering Research* 79 (2): 125-137.

Chen, Y., S. Tessier, C. Cavers, X. Xu and F. Monero. 2004. A survey of crop residue burning practices in Manitoba. *Applied Engineering in Agriculture* 21(3): 317-323.

Chen, Y., L. J. Munkholm, and T. Nyord. 2013a. A discrete element model for soil-sweep interaction in three different soils. *Soil & Tillage Research*, 136: 34-41.

Chi L. and R. Kushwaha. 1990. A non-linear 3-D finite element analysis of soil failure with tillage tools. *Journal of Terramechanics*, 27(4): 343-366.

Coetzee C.J. and D.N.J. Els. 2009. Calibration of discrete element parameters and the modelling of silo discharge and bucket filling. *Computers and Electronics in Agriculture* 65: 198-212.

Collins, B.A. and D.B. Fowler. 1996. Effect of soil characteristics, seeding depth, operating speed, and opener design on draft force during direct seeding. *Soil & Tillage Research* 39(3-4): 199-211.

Conte, O., R. Levien, H. Debiasi, S.L.K. Stürmer, M. Mazurana and J. Müller. 2011. Soil disturbance index as an indicator of seed drill efficiency in no-tillage agrosystems. *Soil & Tillage Research* 114: 37-42.

Cundall, P.A. and O.D.L. Strack. 1979. A discrete numerical model for granular assemblies. *Geotechnique* 29: 47-55.

Darmora, D.P., Pandey, K.P., 1995. Evaluation of performance of furrow openers of combined seed and fertiliser drills. *Soil & Tillage Research* 34(2), 127–139.

Doan, V., Y. Chen and B. Irvine. 2005. Effect of oat stubble height on the performance of no-till seeder openers. *Canadian Biosystems Engineering* 47: 2.37-2.44.

Fielke, J., M. Ucgul and C. Saunders. 2013. Discrete element modeling of soil-implement interaction considering soil plasticity, cohesion and adhesion. ASABE Paper No. 131618800. St. Joseph, MI: ASABE.

Gao, Q., Y. Chen, H. Zhou and M.A. Sadek. 2015. Simulation of soil dynamic properties of a seed opener using the discrete element method (DEM). *Agricultural Engineering International: CIGR Journal* 17(3): 72-82.

Godwin, R.G. and G. Spoor. 1977. Soil failure with narrow tines. *Journal of Agricultural Engineering Research* 22: 213-228.

Gratton, J., Y. Chen and S. Tessier. 2003. Design of a spring-loaded downforce system for a no-till seed opener. *Canadian Biosystems Engineering* 45: 2.29-2.35.

Green, M. and D. Poisson. 1999. Residue management for successful direct seeding. Agdex 580-40. Alberta, Canada: Alberta Agriculture, Food and Rural Development.

Hasimu, A. and Y. Chen. 2014. Soil disturbance and draft force of selected seed openers. *Soil & Tillage Research* 140: 48-54.

Hettiaratchi, D.R.P., B.D. Witney and A.R. Reece. 1966. The calculation of passive pressure in two-dimensional soil failure. *Journal of Agricultural Engineering Research* 11(2): 89-107.

Itasca, 2015. Particle flow code in 3 dimensions (PFC3D). Theory and Background. Itasca consulting group, Inc., Minneapolis, Minnesota, USA.

Janelle, L., S. Tessier and C. Laguë. 1995. Seeding tool design for no-tillage conditions in north-eastern America. ASAE Paper No. 93-1561. St. Joseph, MI: ASAE.

Karmakar S., R.L. Kushwaha and C. Laguë. 2007. Numerical modelling of soil stress and pressure distribution on a flat tillage tool using computational fluid dynamics. *Biosystems Engineering* 97(3): 407-414.

Land Resource Unit. 1999. Soils and terrain. An introduction to the land resource. Rural municipality of Macdonald. Information bulletin 98-25.

Landry H., C. Laguë and M. Roberge. 2006. Discrete element modeling of machine-manure interactions. *Computers and Electronics in Agriculture* 52(1-2): 90-106.

Li, B., Y. Chen and J. Chen. 2016. Modeling of soil-claw interaction using the Discrete Element Method (DEM). *Soil & Tillage Research* 158: 177-185.

Liu, J., D.A. Lobb, Y. Chen and R. L. Kushwaha. 2008. Steady-state models for the movement of soil and straw during tillage with a single sweep. *Transactions of the ASABE* 51(3): 781-789.

Lim, W.L. and G.R. McDowell. 2008. A limit analysis of the kinematics of void collapse using the discrete element method. *Geomechanics and Geoengineering: An International Journal* 3(1): 41-58.

Lu, Z., S.C. Negi and J.C. Jofriet. 1997. A numerical model for flow of granular materials in silos. Part 1: model development. *Journal of Agricultural Engineering Research* 68: 223-229.

Mahadi M R. 2005. Development of a soil bin test facility for soil dynamics studies. M.Sc. thesis. Winnipeg, MB: Department of Biosystems Engineering, University of Manitoba.

Mak, J. 2011. Rolling tines - evaluation and simulation using discrete element method. M. Sc. thesis. Winnipeg, MB: Department of Biosystems Engineering, University of Manitoba.

Mak**,** J. and Y. Chen. 2014. Simulation of draft forces of a sweep in a loamy sand soil using the discrete element method. *Canadian Biosystems Engineering* 56: 2.1-2.7.

Mak, J., Y. Chen, and M. A. Sadek. 2012. Determining parameters of a discrete element model for soil–tool interaction. *Soil & Tillage Research* 118: 117–122.

McKyes, E. 1985. *Soil Cutting and Tillage*. New York, NY. Elsevier.

McKyes, E. and O.S. Ali. 1977. The cutting of soil by narrow blades. *Journal of Terramechanics* 14(2): 43-58.

Murray, S. 2014. Analysis of the performance of disc openers for granular fertilizer application. B.Sc. thesis. Winnipeg, MB: Department of Biosystems Engineering, University of Manitoba.

Nalavade P, V. Salokhe, T. Niyamapa, and P. Soni. 2010. Performance of free rolling and powered tillage discs. *Soil & Tillage Research* 109:87 – 93.

Nandanwar, M. 2015. Measurement and simulation of triaxial compression tests for a sandy loam soil. M.Sc. thesis. Winnipeg, MB: Department of Biosystems Engineering, University of Manitoba.

Parent, G., S. Tessier, G. Allard and D.A. Angers. 1993. Seedbed characteristics for forages and cereals with no-tillage in the northeast. ASAE Paper No. 93-1562. ASAE, St. Joseph, MI.

Plouffe, C., M.J. Richard, S. Tessier and C. Laguë. 1999. Validations of moldboard plow simulations with FEM on a clay soil. *Transactions of the ASAE* 42(6): 1523-1529.

Potyondy, D.O. and P.A. Cundall. 2004. A bond-particle model for rock. *International Journal of Rock Mechanics & Mining Science* 41: 1392-1364.

Rahman, S., Y. Chen and D. Lobb. 2005. Soil movement resulting from sweep type manure injection tools. *Biosystems Engineering* 91(3): 379-392.

Rathore, T.R., B.P. Ghildyal and R.S. Sachan. 1981. Germination and emergence of soybean under crusted soil conditions. *Plant Science* 62: 97–105.

Sadek, M.A. and Y. Chen. 2015. Feasibility of using PFC^{3D} to simulate soil flow resulting from a simple soil engaging tool. *Transactions of the ASABE* 58(4): 987-996.

Sadek, M.A., Y. Chen, and J. Liu. 2011. Simulating shear behavior of a sandy soil under different soil conditions. *Journal of Terramechanics* 48: 451-458.

Srivastava, A.K., C.E. Goering, R.P. Rohrbach and D.R. Buckmaster. 2006. *Engineering Principles of Agricultural Machines,* 2^{nd} Edition. St. Joseph, MI: ASABE.

Tamás K., I. J. Jóri, and A. M. Mouazen. 2013. Modelling soil–sweep interaction with discrete element method. *Soil & Tillage Research* 134(11): 223–231.

Tamet, V., J. Boiffin, C. Dürr and N. Souty. 1996. Emergence and early growth of an epigeal seedling (daucus carota l.): influence of soil temperature, sowing depth, soil crusting and seed weight. *Soil & Tillage Research* 40(1-2) 25 – 38.

Tanaka, H., A. Oida, M. Daikoku, K. Inooku, O. Sumikawa, Y. Nagasaki and M. Miyazaki. 2007. DEM simulation of soil loosening process caused by a vibrating subsoiler. *Agricultural Engineering International: the CIGR Ejournal* Vol. IX, Manuscript PM 05 010.s

Upadhyaya, S.K., U.A. Rosa and D. Wulfshon. 2000. Application of finite element method in agricultural soil mechanics. In *Advances in Soil Dynamics*, Vol II. St. Joseph, MI: ASABE.

van der Linde, J. 2007. Discrete element modelling of a vibratory subsoiler. Matieland, South Africa: M.Sc. Thesis, Department of Mechanical and Mechatronic Engineering, University of Stellenbosch.